

NASA/TP-2007-215086



Refinement of Timoshenko Beam Theory for Composite and Sandwich Beams Using Zigzag Kinematics

*Alexander Tessler
Langley Research Center, Hampton, Virginia*

*Marco Di Sciuva and Marco Gherlone
Department of Aeronautics and Space Engineering
Politecnico di Torino, Torino, Italy*

November 2007

The NASA STI Program Office . . . in Profile

Since its founding, NASA has been dedicated to the advancement of aeronautics and space science. The NASA Scientific and Technical Information (STI) Program Office plays a key part in helping NASA maintain this important role.

The NASA STI Program Office is operated by Langley Research Center, the lead center for NASA's scientific and technical information. The NASA STI Program Office provides access to the NASA STI Database, the largest collection of aeronautical and space science STI in the world. The Program Office is also NASA's institutional mechanism for disseminating the results of its research and development activities. These results are published by NASA in the NASA STI Report Series, which includes the following report types:

- **TECHNICAL PUBLICATION.** Reports of completed research or a major significant phase of research that present the results of NASA programs and include extensive data or theoretical analysis. Includes compilations of significant scientific and technical data and information deemed to be of continuing reference value. NASA counterpart of peer-reviewed formal professional papers, but having less stringent limitations on manuscript length and extent of graphic presentations.
- **TECHNICAL MEMORANDUM.** Scientific and technical findings that are preliminary or of specialized interest, e.g., quick release reports, working papers, and bibliographies that contain minimal annotation. Does not contain extensive analysis.
- **CONTRACTOR REPORT.** Scientific and technical findings by NASA-sponsored contractors and grantees.

- **CONFERENCE PUBLICATION.** Collected papers from scientific and technical conferences, symposia, seminars, or other meetings sponsored or co-sponsored by NASA.
- **SPECIAL PUBLICATION.** Scientific, technical, or historical information from NASA programs, projects, and missions, often concerned with subjects having substantial public interest.
- **TECHNICAL TRANSLATION.** English-language translations of foreign scientific and technical material pertinent to NASA's mission.

Specialized services that complement the STI Program Office's diverse offerings include creating custom thesauri, building customized databases, organizing and publishing research results ... even providing videos.

For more information about the NASA STI Program Office, see the following:

- Access the NASA STI Program Home Page at <http://www.sti.nasa.gov>
- E-mail your question via the Internet to help@sti.nasa.gov
- Fax your question to the NASA STI Help Desk at (301) 621-0134
- Phone the NASA STI Help Desk at (301) 621-0390
- Write to:
NASA STI Help Desk
NASA Center for AeroSpace Information
7115 Standard Drive
Hanover, MD 21076-1320

NASA/TP-2007-215086



Refinement of Timoshenko Beam Theory for Composite and Sandwich Beams Using Zigzag Kinematics

Alexander Tessler
Langley Research Center, Hampton, Virginia

Marco Di Sciuva and Marco Gherlone
Department of Aeronautics and Space Engineering
Politecnico di Torino, Torino, Italy

National Aeronautics and
Space Administration

Langley Research Center
Hampton, Virginia 23681-2199

November 2007

The use of trademarks or names of manufacturers in this report is for accurate reporting and does not constitute an official endorsement, either expressed or implied, of such products or manufacturers by the National Aeronautics and Space Administration.

Available from:

NASA Center for AeroSpace Information (CASI)
7115 Standard Drive
Hanover, MD 21076-1320
(301) 621-0390

National Technical Information Service (NTIS)
5285 Port Royal Road
Springfield, VA 22161-2171
(703) 605-6000

Abstract

A new refined theory for laminated-composite and sandwich beams that contains the kinematics of the Timoshenko Beam Theory as a proper baseline subset is presented. This variationally consistent theory is derived from the virtual work principle and employs a novel piecewise linear zigzag function that provides a more realistic representation of the deformation states of transverse shear flexible beams than other similar theories. This new zigzag function is unique in that it vanishes at the top and bottom bounding surfaces of a beam. The formulation does not enforce continuity of the transverse shear stress across the beam's cross-section, yet is robust. Two major shortcomings that are inherent in the previous zigzag theories, shear-force inconsistency and difficulties in simulating clamped boundary conditions, and that have greatly limited the utility of these previous theories are discussed in detail. An approach that has successfully resolved these shortcomings is presented herein. Exact solutions for simply supported and cantilevered beams subjected to static loads are derived and the improved modelling capability of the new "zigzag" beam theory is demonstrated. In particular, extensive results for thick beams with highly heterogeneous material lay-ups are discussed and compared with corresponding results obtained from elasticity solutions, two other "zigzag" theories, and high-fidelity finite element analyses. Comparisons with the baseline Timoshenko Beam Theory are also presented. The comparisons clearly show the improved accuracy of the new, refined "zigzag" theory presented herein over similar existing theories. This new theory can be readily extended to plate and shell structures, and should be useful for obtaining relatively low-cost, accurate estimates of structural response needed to design an important class of high-performance aerospace structures.

Nomenclature

$A, 2h, L$	beam's cross-sectional area, depth, and span
$2h^{(k)}$	thickness of the k -th layer
q, F	transverse pressure [force/length] and force loading
(T_{xq}, T_{zq})	axial and shear tractions prescribed at the ends of beam x_q ($q = a, b$)
$(u_x^{(k)}, u_z^{(k)})$	axial and transverse components of the displacement vector in the k th layer
(u, θ, ψ, w)	kinematic variables of zigzag theory

$\phi^{(k)}$	zigzag function
$(\varepsilon_x^{(k)}, \gamma_{xz}^{(k)})$	axial and transverse shear strain in the k -th layer
$(\sigma_x^{(k)}, \tau_{xz}^{(k)})$	axial and transverse shear stress in the k -th layer
$(E_x^{(k)}, G_{xz}^{(k)})$	axial and shear modulus of the k -th layer
λ_A, λ_0	penalty factors
$\xi^{(k)}$	local (k -th layer) thickness coordinate
$u^{(k)}$	normalized axial displacement along the interface between the k -th and $(k + 1)$ layers
$(N_x, M_x, M_\phi, V_x, V_\phi)$	stress resultants of the refined zigzag beam theory
$A_{pq}, B_{pq}, D_{pq},$ and Q_{ij}^λ	constitutive stiffness coefficients of the refined zigzag beam theory
N	number of material layers through the beam's depth

1. Introduction

Performance and weight advantages of advanced composite materials have led to their sustained and increased application to military and civilian aircraft, aerospace vehicles, naval, and civil structures. To design efficient and reliable laminated-composite structures, improved analytical and computational methods that accurately incorporate the principal non-classical effects are necessary. In relatively thick beams, and even in thinner beams that are highly heterogeneous, transverse shear deformation may substantially influence design-significant response quantities such as normal stresses, deflections, and vibration modes and natural frequencies. For this class of problems, classical deformation theories are generally less than adequate. This shortcoming is particularly pronounced in relatively thick laminated-composite and sandwich structures with material layers that exhibit large differences in the transverse shear properties. Application of classical theories in this context often leads to non-conservative predictions for deformation, stresses, and natural frequencies. Moreover, in classical shear deformation models, transverse shear stresses fail to satisfy equilibrium conditions at the layer interfaces, resulting in excessively erroneous discontinuities in these quantities. The two fundamental assumptions of the classical Bernoulli-Euler Beam Theory are that the transverse shear and through-the-depth normal strains are negligible, compared to the axial strain associated with bending action. These assumptions have been shown to be valid for the bending of very slender beams. As a result, the bending deformation may be characterized by a single deflection variable. However, Hooke's law yields a zero-valued transverse shear stress, which violates equilibrium of the internal forces acting within a beam. To rectify this inconsistency in the classical Bernoulli-Euler Beam Theory, a beam equilibrium equation is used to obtain the internal transverse shear force from which an average shear stress is computed. Timoshenko [1] derived a new beam theory by adding an additional kinematic variable in the displacement assumptions, the bending rotation, and a shear correction factor to provide a first-order account of shear deformation in an average sense, while retaining the assumption that the through-the-depth normal strain is negligible. This modification to the kinematics allows the transverse shear stresses to be obtained from Hooke's law and extends the range of applicability of the resulting theory to moderately thick beams and higher vibration frequencies associated with short wave length modes.

The Timoshenko Beam Theory (TBT) and analogous shear-deformation theories for plate and shell structures have been widely used in structural analysis of homogeneous and laminated-composite structures. This theory produces inadequate predictions, however, when applied to relatively thick laminated composites with material layers that have highly dissimilar stiffness characteristics. Even with a judiciously chosen shear correction factor, which is dependent on the laminate stacking sequence, the TBT tends to underestimate, often substantially, the axial stresses at the top and bottom, outer fibers of a beam. Moreover, along the layer interfaces of a laminated-composite beam, the transverse shear stresses predicted often exhibit excessively erroneous discontinuities. The reason for these difficulties is likely associated with the higher complexity of the "true" variation of the displacement field across a highly heterogeneous beam cross-section. Clearly, the linear through-thickness displacement assumption for the axial displacement is the main shortcoming of the TBT when it is applied to complex material systems with significant transverse shear flexibility.

The need for beam, plate, and shell theories with better predictive capabilities has led to the development of the so-called *higher-order theories* that are also commonly known as *refined equivalent single-layer theories* (for a review of many of such theories, refer to [2]). In these refined theories, higher-order kinematic terms, with respect to the beam-depth or shell-thickness coordinate, have been added to the expressions for the in-plane displacements and, in some cases, to the expressions for the transverse displacement. While notable response improvements have been achieved with several of these

theories, they are generally inadequate for predicting the correct shear and axial stresses in, and the high-frequency dynamic responses of, highly heterogeneous laminated-composite and sandwich structures that are moderately thick. Because of these shortcomings, refined theories that incorporate deformation characteristics of the individual layers of the structure have been developed and are commonly referred to as *layer-wise theories*. Notable early contributions to these theories were made by Ambartsumian [3] and by Sun and Whitney [4].

In general, *layer-wise theories* presume that the laminate deformation and stress fields depend significantly on the behavior of the individual layers. In these theories, the layer kinematics are independently described and certain physical continuity requirements are enforced (e.g., refer to the review article in [2]). More specifically, the layer-wise representation of the kinematics yields zigzag-like displacements through the beam depth or shell thickness. Moreover, the increased kinematic freedom enables the enforcement of stress continuity conditions at the layer interfaces. The major drawback of these theories, however, is that the number of kinematic variables is dependent on the number of layers in the beam or shell. This attribute typically results in a great number of solution variables which makes the general layer-wise theories computationally unattractive and, as a result, detracts from their usefulness. Moreover, these theories are particularly cumbersome to implement within a displacement-based finite element method. For further discussions on the merits and drawbacks of general layer-wise theories, refer to [5].

The so-called *zigzag theories* are an important special sub-class of the general layer-wise theories that appear to be amenable to engineering practice. These theories also assume a zigzag pattern for the in-plane displacements and enforce continuity of the transverse shear stresses across the entire laminated-beam depth or laminated-shell thickness. Importantly, the number of kinematic variables in these special layer-wise theories is independent of the number of layers. Early works on the zigzag theories were presented by Di Sciuva [6-8] and Murakami [9] for the bending of plates. Di Sciuva [10-11] also demonstrated that zigzag theories are generally well-suited for finite element implementation.

In Di Sciuva's earlier efforts on plates [6-7], a piecewise linear inplane-displacement function is added to a first-order shear deformation theory (FSDT) in which the transverse shear strains are used as the primary kinematic variables instead of the bending rotations. This piecewise linear function, and others like it, are referred to herein as a "zigzag" function. To retain only the kinematic variables of the FSDT, Di Sciuva enforced a constant shear stress across the entire laminate thickness. This procedure led to the desired enhancement in the representation of the inplane displacement fields and simultaneously achieved transverse shear stress continuity along layer interfaces. An important characteristic of Di Sciuva's formulation is that, when the zigzag function vanishes for homogeneous plates, the theory is reduced to the FSDT baseline. Later, Di Sciuva [12-13] introduced additional enhancements to his zigzag model by adding a cubic in-plane displacement to the zigzag function. It is important to note that the Di Sciuva theories require C^1 -continuous shape functions for formulating suitable finite elements. These approximation schemes are significantly less attractive, especially for plate and shell finite elements, than the C^0 -continuous displacement interpolation schemes associated with FSDTs.

With the goal of obtaining C^0 -continuous finite elements, Averill explored the new linear [14] and cubic [15] zigzag beam models. In particular, Averill modified Di Sciuva's approach by using the TBT as his underlying baseline theory, adding an additional kinematic variable associated with a zigzag function, and by introducing an ad hoc penalty term to the variational principle. The penalty term enforces continuity of the transverse shear stress across the beam cross-section in a limiting sense as the penalty parameter approaches a large value.

Di Sciuva's theory runs into theoretical difficulties with regard to the physical significance of the transverse shear stress associated with the theory. The difficulty is especially evident at a clamped

support, where the cross-sectional area integral of the shear stress, obtained from constitutive relations, does not correspond to the total shear force required by equilibrium. Thus, the correct shear force and the average shear stress must be determined from the equilibrium equation that relates the shear force to the derivative of the bending moment, as in the Bernoulli-Euler Beam Theory. Averill's theory also suffers from its inability to model correctly a clamped boundary condition, where it predicts erroneously that the transverse shear stress and the corresponding resultant force vanish. To alleviate this anomaly, Averill proposed a boundary condition compromise at the expense of variational consistency of the theory, in which a kinematic variable representing the amplitude of the zigzag displacement is left out of the variationally required set of boundary conditions. Consequently, extensive analytic and numerical studies that have been conducted primarily focused on beams and plates with simply supported boundaries [6, 7, and 12-15]. Recently, a zigzag plate analysis was discussed for clamped plates [16]; however, no results were presented for the shear stresses at a clamped edge.

Scrutiny of the zigzag theories discussed herein has revealed some serious shortcomings. The objective of the present study is to present a new refined zigzag theory that is free of these shortcomings and amenable to finite element implementation. In particular, the present paper discusses a new *refined zigzag* beam theory that is consistently derived from the virtual work principle, by refining the ideas of Timoshenko, Di Sciuva, and Averill. The key attributes of the present theory are, first, the proposed zigzag function vanishes at the top and bottom surfaces of the beam and does not require full shear-stress continuity across the laminated-beam depth. Second, all boundary conditions, including the fully clamped condition, can be modeled adequately. And third, the theory only requires C^0 -continuous kinematics for finite element modeling, as do elements based on the theories of Timoshenko [1], Mindlin [17], and Reissner [18]. This latter attribute lends itself to developing computationally efficient and robust beam, plate, and shell finite elements. Overall, the theory appears as a natural extension of the TBT to laminated-composite beams, and it is devoid of the drawbacks of the zigzag theories discussed previously.

In the remainder of the report, the concept of zigzag kinematic assumptions is first described. Then the zigzag schemes of Di Sciuva and Averill are elaborated in detail, and their deficiencies with respect to the transverse shear properties and clamped boundary conditions are highlighted. A unique zigzag function is then introduced to formulate the basis for the refined zigzag theory, giving rise to the transverse shear stress that has a piecewise constant distribution across the laminate thickness. As an added explanation of the underlying reasons for the drawbacks of Averill's formulation, a penalized form of the constitutive equations is introduced within the present theory. The equations of equilibrium and associated boundary conditions are then derived from the virtual work principle. Finally, the refined zigzag theory is assessed quantitatively by way of exact solutions for simply supported and cantilevered composite and sandwich beams. Thick beams composed of highly heterogeneous material lay-ups are considered. Comparisons are made with several beam theories, exact elasticity solutions, and results obtained with high-fidelity, two-dimensional elasticity finite element models.

2. Basis for Zigzag Kinematics

Laminated-composite beams are generally made of relatively thin layers of different materials, with different fiber orientations, that may have significantly different degrees of axial compliance. As a result, the axial displacement distribution of these heterogeneous, anisotropic beams exhibit varies in a nonlinear manner along the depth of the beam cross-section, especially for relatively deep beams with low slenderness ratios. Moreover, the axial displacement distribution is likely to exhibit a discontinuity in slope along the layer interfaces when the compliance of two contiguous layers is substantially different. Within each layer, the axial displacement distribution is presumed to be continuous, with continuous

slopes, consistent with the usual representation of the fibers and matrix material as a homogeneous layer. In a general layer-wise formulation of a beam theory, the axial displacement field could be modeled as a piecewise continuous function that is a collection of given nonlinear functions defined for each layer. However, if the beam stacking sequence is modeled as a collection of layers with layer thicknesses that are thin compared to the characteristic beam depth, then it is reasonable to presume that the nonlinear axial displacement distribution can be adequately modeled as a piecewise continuous function that is a collection linear functions defined for each layer. A function of this type is referred to herein as a “zigzag” function and, as a result, the corresponding beam theory is referred to as a Zigzag Beam Theory. Another important consideration, not addressed herein, is that if delaminations along given layer interfaces are present, a zigzag function with jump discontinuities at the given layer interfaces [20] could be used to represent the delaminations.

Observations such as these have been substantiated by exact elasticity solutions such as that of Pagano [19]. Efforts like Pagano’s prompted Di Sciuva [7] to formulate a refined plate theory in which a zigzag function is added to a special form of FSDT in which the shearing strains are used as independent variables. In this special formulation, the total rotations (the first derivatives of the deflection variable) provide the through-the-thickness linear distributions of the axial displacements, as in the classical Kirchhoff-Love plate and shell theories. Following Di Sciuva’s work, Averill [14] proposed a similar zigzag formulation for the bending analysis of laminated-composite beams. In contrast, Averill’s formulation uses the standard form of TBT in which the bending rotation is the independent variable appearing in the kinematics for the axial displacement. However, both of these formulations have some undesirable attributes. In what follows, the essential aspects of the Di Sciuva and Averill zigzag models are examined in order to set the stage for the new *refined zigzag* beam-bending theory presented herein.

2.1 Problem Formulation and Kinematics

The basic problem of the present study is a narrow beam with depth of $2h$ and cross sectional area A that undergoes only plane deformations. The beam is made of N orthotropic-material layers that are perfectly bonded to each other, and the major principal material axis of each layer is parallel to the centrally located beam x axis shown in Figure 1. Static loads are considered which generally include a distributed transverse line load $q(x)$ (force/length) and prescribed axial (T_{xa} , T_{xb}) and shear (T_{za} , T_{zb}) tractions at the two reference cross sections, $x = x_a$ and x_b , shown in Figure 1. Material points of the beam are located, prior to deformation, by the coordinates (x, z) , where $x \in [x_a, x_b]$ and $z \in [-h, h]$.

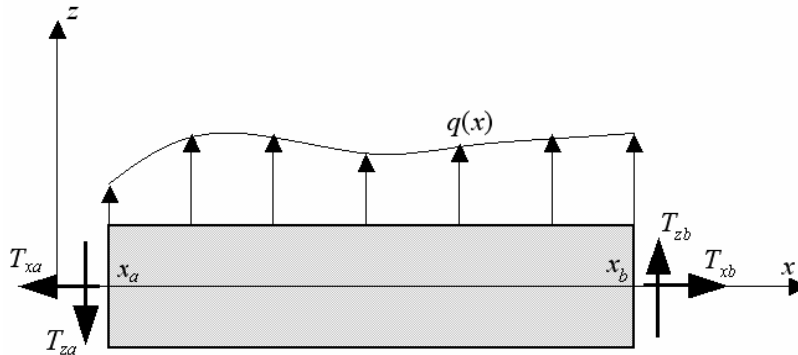


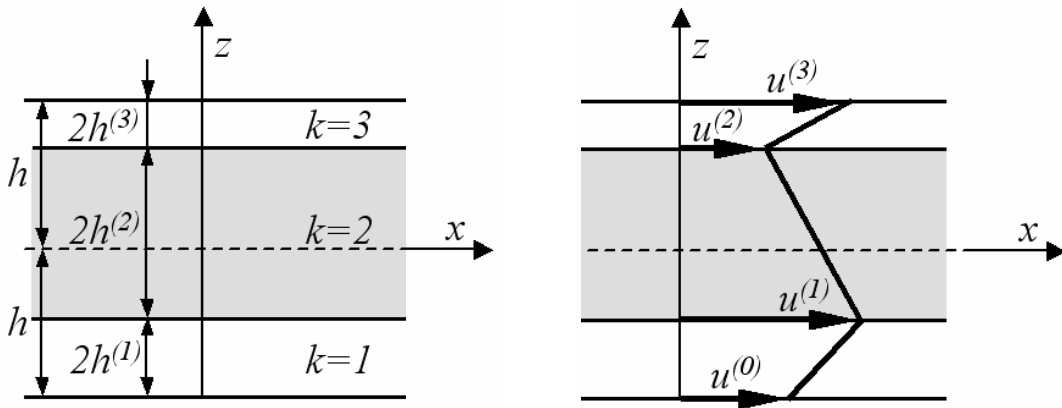
Figure 1. Beam subjected to transverse loading and end tractions.

For material points within the k -th layer of a laminated-composite beam, the through-the-depth coordinates are given by $z \in [z_{(k)}, z_{(k+1)}]$, where $k = 1, \dots, N$. An expression for the beam displacements, that is general enough to describe the kinematics of the Di Sciuva, Averill, and present *refined zigzag* theories, is given by

$$\begin{aligned} u_x^{(k)}(x, z) &= u(x) + z\theta(x) + \phi^{(k)}(z)\psi(x) \\ u_z^{(k)}(x, z) &= w(x) \end{aligned} \quad (1)$$

where the superscript (k) indicates $z_{(k)} \leq z \leq z_{(k+1)}$. In Eq. (1), the uniform axial displacement, $u(x)$, the bending rotation, $\theta(x)$, and the transverse deflection, $w(x)$, are the primary kinematic variables of the underlying equivalent single-layer beam theory. The symbol $\phi^{(k)}(z)$ denotes a piecewise linear *zigzag* function, yet to be established, and $\psi(x)$ is a primary kinematic variable that defines the amplitude of the zigzag function along a beam. When dynamic effects are considered, the four primary kinematic variables defined by Eq. (1) are also functions of time. If either $\phi^{(k)}(z) = 0$ or $\psi(x) = 0$, the kinematic assumptions of Eq. (1) correspond to the TBT, if the rotation $\theta(x)$ is a primary kinematic variable. Note that depending on the specific FSDT theory used for the baseline kinematics, the four kinematic variables may have slightly different physical interpretations.

The notations used in the present study together with a general distribution for the zigzag function are shown for a three-layer beam in Figure 2. The $N + 1$ axial displacements at the layer interfaces and the outer beam surfaces, as illustrated for $N = 3$ in Figure 2, are denoted herein for an N -layer laminate by $u^{(0)}, u^{(1)}, \dots, u^{(N)}$. Collectively, this set of displacements is referred to herein as the interfacial displacements even though $u^{(0)}$ and $u^{(N)}$ are not at the interface of two adjacent layers.



(a) Layer notation for a three-layer laminate.

(b) Zigzag function defined in terms of the interfacial axial displacements, $u^{(i)}$ ($i = 0, 1, \dots, N$).

Figure 2. Layer notation for a three-layer laminate and a corresponding generic zigzag function.

The linear strain-displacement relations of elasticity theory and the displacements defined by Eq. (1) give rise to the nonzero strain expressions

$$\begin{aligned}\varepsilon_x^{(k)}(x, z) &\equiv u_{x,x}^{(k)} = u_{,x} + z \theta_{,x} + \phi^{(k)} \psi_{,x} \\ \gamma_{xz}^{(k)}(x, z) &\equiv u_{x,z}^{(k)} + u_{z,x}^{(k)} = \gamma + \beta^{(k)} \psi\end{aligned}\quad (2)$$

where $\beta^{(k)} \equiv \phi_{,z}^{(k)}$, and $\gamma \equiv w_{,x} + \theta$ represents the average shearing strain (or shearing angle) of the TBT. Note that, since $\phi^{(k)}(z)$ is piecewise linear, $\beta^{(k)}$ is a piecewise constant function, i.e., it is constant across each material layer. For major principal material axes that are coincident with beam x axis, Hooke's stress-strain relations for the k -th orthotropic layer have the standard form

$$\begin{Bmatrix} \sigma_x^{(k)} \\ \tau_{xz}^{(k)} \end{Bmatrix} = \begin{bmatrix} E_x^{(k)} & 0 \\ 0 & G_{xz}^{(k)} \end{bmatrix} \begin{Bmatrix} \varepsilon_x^{(k)} \\ \gamma_{xz}^{(k)} \end{Bmatrix}\quad (3)$$

where $E_x^{(k)}$ and $G_{xz}^{(k)}$ denote the axial and shear moduli of the k -th layer, respectively.

To facilitate subsequent discussions, it is convenient to define a ‘‘difference function’’ $\eta(x)$ as

$$\eta \equiv \gamma - \psi\quad (4)$$

This definition leads to the following convenient expressions for the transverse shear strain and shear stress in terms of the $\gamma(x)$ and $\eta(x)$ functions

$$\gamma_{xz}^{(k)} = (1 + \beta^{(k)})\gamma - \beta^{(k)}\eta\quad (5)$$

$$\tau_{xz}^{(k)} = G_{xz}^{(k)}(1 + \beta^{(k)})\gamma - G_{xz}^{(k)}\beta^{(k)}\eta\quad (6)$$

2.2 Di Sciuva's zigzag model

Di Sciuva's zigzag model [7] was originally developed for plate bending. The corresponding beam kinematics is obtained from Eqs. (1) by using the variable substitutions

$$\theta = \psi - w_{,x}\quad (7)$$

and replacing z in Eqs. (1) with $(z + h)$. Thus, the axial displacement of Di Sciuva's model has the form

$$u_x^{(k)}(x, z) = u(x) + (z + h)[\psi(x) - w_{,x}(x)] + \phi_{DS}^{(k)}(z) \psi(x)\quad (8)$$

where the transverse displacement is the same as in the second of Eqs. (1), and where $\phi_{DS}^{(k)}$ now designates the actual form of the zigzag function used by Di Sciuva. These kinematics give rise to shear strain and stress that are piecewise constant (i.e., constant within each layer) and which are defined exclusively in terms of the amplitude function ψ as follows

$$\begin{aligned}\gamma_{xz}^{(k)} &= (1 + \beta_{DS}^{(k)})\psi \\ \tau_{xz}^{(k)} &= G_{xz}^{(k)}(1 + \beta_{DS}^{(k)})\psi\end{aligned}\tag{9}$$

To determine the function $\phi_{DS}^{(k)}$, Di Sciuva enforced a specific set of stress-continuity constraints along the layer interfaces that require all layers have the same (constant) transverse shear stress, that is,

$$\tau_{xz}^{(k)} = \tau_{xz}^{(k+1)}, \quad k = 1, \dots, N-1\tag{10}$$

Since Eqs. (10) impose only $N-1$ constraints, and there are $N+1$ interfacial displacements needed to define $\phi_{DS}^{(k)}$, the zigzag function is specified to vanish across the entire bottom layer ($u^{(0)} = u^{(1)} = 0$), as illustrated in Figure 3(a). More generally, it is straightforward to select any given layer in which the zigzag function is specified to vanish [20]. Henceforth, determining a zigzag function by specifying (or fixing) a single layer contribution to vanish is referred to herein as a *fixed-layer zigzag function method*.

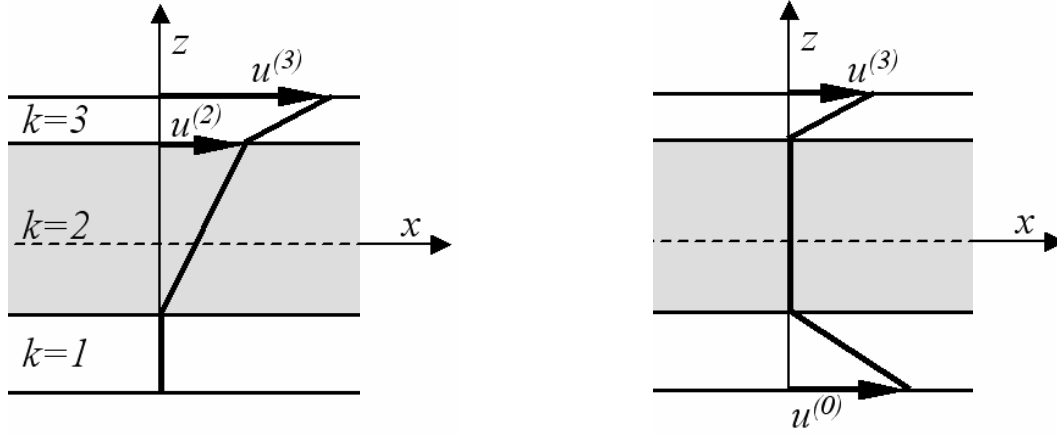
The transverse shear stress distribution that results from Di Sciuva's kinematics is uniform through the beam depth. If fixing the first layer ($k=1$) is used to define the zigzag function ($\phi_{DS}^{(1)} = \beta_{DS}^{(1)} = 0$), as depicted in Figure 3(a), then the definition of ψ as the shear strain in the first layer becomes evident from Eqs. (9); that is,

$$\psi = \gamma_{xz}^{(1)}\tag{11}$$

In addition, the transverse shear stress in all layers simply equals that in the first layer and are given by

$$\tau_{xz}^{(k)} = G_{xz}^{(1)} \gamma_{xz}^{(1)} \quad (k = 1, \dots, N)\tag{12}$$

An undesirable consequence of Di Sciuva's approach to defining the zigzag function is the counterintuitive result that the transverse shear stresses in all layers are identical and equal to that in the layer that is specified to have zero-valued interfacial displacements. Moreover, the shear modulus of this fixed layer serves as a single weighting coefficient for the entire shear strain energy, which produces a bias in the deformation model toward the shear stiffness of the fixed layer. In contrast, $\phi_{DS}^{(k)}$ should depend on all shear moduli $G_{xz}^{(k)}$, and layer thicknesses, $2h^{(k)}$. The key property of Di Sciuva's model is that the zigzag function vanishes identically for homogeneous beam, in which case the theory reverts to the underlying shear-deformation theory. The improved predictive capability of the model due to the $\phi_{DS}^{(k)} \psi$ term in Eq. (1) is particularly appreciable for thick and highly heterogeneous laminates.



(a) Di Sciuva's zigzag-function distribution [7].

(b) Averill's zigzag-function distribution [14].

Figure 3. Di Sciuva's and Averill's zigzag-function distributions.

Di Sciuva's zigzag model exhibits another theoretical difficulty associated with the physical interpretation of the uniform transverse shear stress distribution that results from the procedure that defines its zigzag function. In particular, the physically correct shear force $V_x(x)$ obtained from the well-established equilibrium equation for beams

$$V_x = M_{x,x} \quad (13)$$

is different from the corresponding force that is obtained when the shear stress in Eq. (12) is integrated over the cross-section, that is,

$$V_x \neq \int_A \tau_{xz}^{(k)} dA = A \tau_{xz}^{(1)} \quad (14)$$

A related difficulty arises for a clamped support condition. For this case, the variationally consistent displacement boundary conditions are given as

$$u = w = w_{,x} = \psi = 0 \quad (15)$$

Because $\psi = 0$ is required at a clamped end, the corresponding transverse shearing strain and stress defined in Eqs. (9) vanish identically. In contrast, a non vanishing average shear stress $\tau_{xz} = V_x / A$ at a clamped end is given by the shear force obtained from the equilibrium equation given by Eq. (13).

From the perspective of finite element approximations appropriate for this type of beam theory, $w(x)$ needs to be at least C^1 continuous, since the axial strain is proportional to the second derivative of $w(x)$. This requirement yields an added impediment for the approximation functions, particularly in developing efficient plate and shell elements based on this type of theory. It has been shown, however, that C^0 continuous kinematic approximations, usually associated with the FSDTs of Timoshenko [1], Mindlin

[17] and Reissner [18], result in simpler, computationally more efficient, and better performing finite elements than comparable elements based on C^1 continuous interpolations. It is this practical aspect that motivated Averill [14] to introduce a different zigzag model.

2.3 Averill's Zigzag Model

Averill [14] developed a zigzag model for laminated-beam deformation that utilizes a penalty method that enforces the continuity of the transverse shear stress across the laminate depth in a limited sense. In this model, the standard form of TBT is used to provide the kinematics of the underlying equivalent single-layer theory; that is, the bending rotation is a primary kinematic variable in the expression for the axial displacement. The specific expression for the axial displacement used in Averill's model may be expressed as

$$u_x^{(k)}(x, z) = u(x) + (z + h - 2h^{(1)})\theta(x) + \phi_A^{(k)}(z)\psi(x) \quad (16)$$

where $\phi_A^{(k)}$ denotes Averill's zigzag function, which is depicted in Figure 3(b) for a three-layer laminate. This expression is consistent with a zigzag function defined by fixing the interfacial displacements of the second layer ($k = 2$). In Eq. (16), $\theta(x)$ represents the rotation of the second layer, that is, $u_{x,z}^{(2)} = \theta$.

The shear stress continuity conditions given by Eq. (10) are enforced explicitly only on the first term of the shear stress given by Eq. (6). This enforcement is done by defining $G_A \equiv G_{xz}^{(k)}(1 + \beta^{(k)})$ and requiring this quantity to be constant for all material layers. Because the interfacial displacements of the second layer are fixed to define the zigzag function, it follows that $\phi_A^{(2)} = \beta_A^{(2)} = 0$. Thus, it also follows that $G_A = G_{xz}^{(2)}$, and the transverse shear stresses reduce to

$$\tau_{xz}^{(k)} = G_{xz}^{(2)}\gamma - G_{xz}^{(k)}\beta_A^{(k)}\eta \quad (k = 1, \dots, N) \quad (17)$$

where $\gamma = \gamma_{xz}^{(2)}$, the shearing strain in the second (fixed) layer. Further, the second term in Eq. (17) diminishes to zero, in a limiting sense, by enforcing

$$\eta \equiv \gamma - \psi \rightarrow 0 \quad (18)$$

with the aid of the following penalty constraint term which is added to the strain energy

$$I_\lambda \equiv \frac{\lambda_A}{2} \int_{x_a}^{x_b} \eta^2 dx \quad (19)$$

In this equation, λ_A is a penalty factor (units of force) which is set to a large value ($\lambda_A \rightarrow \infty$) to ensure the validity of Eq. (18). Under these conditions, the shear stresses are uniform only in a limiting sense, that is,

$$\tau_{xz}^{(k)} \rightarrow \tau_{xz}^{(k+1)} \rightarrow G_{xz}^{(2)}\gamma \quad (k = 1, \dots, N-1) \quad (20)$$

In addition, the transverse shear force derived from the beam equilibrium equation is not equal to the cross-sectional integral of the transverse shear stress, and is given as

$$V_x \equiv \int_A \tau_{xz}^{(k)} dA + \lambda_A \eta(x) \quad (21)$$

Averill's zigzag model results in a four-variable theory and C^0 - continuous kinematics that are suitable for efficient finite element interpolations. However, the model appears to possess some significant theoretical anomalies. As in Di Sciuva's zigzag model, there is the anomaly associated with specifying the interfacial displacements of a given layer to vanish, which is manifested as a bias toward the shear properties of that layer. This bias means that the methodology for defining the zigzag function lacks invariance with respect to the choice of the fixed layer. Moreover, Averill's model gives erroneous results at a clamped end. More specifically, because a clamped boundary condition requires

$$u = w = \theta = \psi = 0 \quad (22)$$

and the penalty condition given by Eq. (18) yields the additional constraint $w_{,x} \rightarrow 0$, the following erroneous conditions for the shear strain and stress at a clamped end result

$$\left(\gamma_{xz}^{(k)}, \tau_{xz}^{(k)} \right)_{@ \text{clamped support}} \rightarrow 0 \quad (23)$$

Averill recognized this anomaly and proposed to avoid prescribing boundary conditions on the ψ variable, thus violating the variational consistency of the theory.

The theoretical difficulties associated with Di Sciuva's and Averill's zigzag models motivated the development a variationally consistent zigzag model for laminated-composite beams that is devoid of these difficulties. The resulting new theory is presented subsequently and is referred to herein as the *refined zigzag* model.

3. Refined Zigzag Model

In this section, a novel, refined zigzag model for laminated-composite beams is presented that is free of the theoretical difficulties of the Di Sciuva and Averill models. The new model uses the TBT as the underlying equivalent single-layer theory that is obtained when the new zigzag function vanishes. The kinematic assumptions of the new model are given in Eqs. (1), and the corresponding strains and stresses are given in Eqs. (2)-(6). The key advantages of the new refined zigzag model are described subsequently, and the variationally consistent equilibrium equations and boundary conditions are derived from the virtual work principle.

3.1 Zigzag Function

The main difference between the new zigzag function presented herein and those used by Di Sciuva and Averill is that the new zigzag function is prescribed to vanish on the outer surfaces of the laminated

beam instead of within a given layer. This important difference ensures a more physically realistic distribution for the zigzag function. Specifically, the zigzag function distribution is nonzero throughout the beam depth and, as a result, the new zigzag function provides a contribution from each layer to the overall deformation of the beam cross-section. This new zigzag function is illustrated for a three-layer beam in Figure 4.

With this new form of the zigzag function, the axial displacement given by the first of Eqs. (1) may be interpreted as a superposition of a layer-wise correction on to the standard form of TBT. That is, the terms $u(x)$ and $z\theta(x)$ provide the basic, first-order, linear through-the-depth displacement distribution of TBT. Moreover, these terms provide the nonzero displacements at the bottom and top surfaces of the beam, which are zero-valued in the zigzag function; that is,

$$u_x^{(0)} = u(x) - h\theta(x) \text{ and } u_x^{(N)} = u(x) + h\theta(x) \quad (24)$$

The zigzag component of the axial displacement, $\phi^{(k)}\psi(x)$, represents the nonlinear distortion of the beam cross-section within the interior and is defined herein such that

$$\phi^{(k)} \equiv \phi(z, u^{(k)}) \quad (k = 1, \dots, N-1) \quad (25)$$

This definition for the zigzag function is intended to indicate that its through-the-depth variation depends only on the interior displacements at the layer interfaces, as illustrated in Figure 4 for a three-layer laminate.

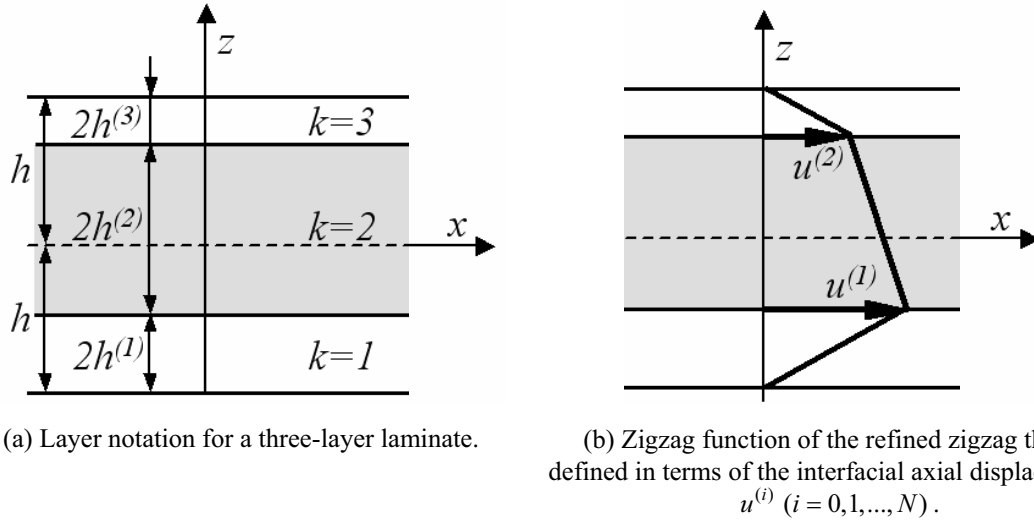


Figure 4. Layer notation for a three-layer laminate and zigzag function of the refined zigzag theory.

With this type of kinematic arrangement, the axial strains at the top and bottom beam surfaces are represented by the TBT contribution to the axial displacement field; that is,

$$\varepsilon_x^{(0)} = u_{,x} - h \theta_{,x} \quad \text{and} \quad \varepsilon_x^{(N)} = u_{,x} + h \theta_{,x} \quad (26)$$

To arrive at a simple representation of the zigzag function, $\phi^{(k)}$, in terms of the layer-interface displacements, $u^{(k)}$, it is convenient to introduce local layer coordinates, $\xi^{(k)}$, that are non-dimensionalized by the corresponding layer thickness, $2h^{(k)}$, such that $\xi^{(k)} \in [-1, 1]$ and $k = 1, \dots, N$. These local thickness coordinates are defined in terms of the N -layer-laminate thickness coordinate $z \in [-h, h]$ as

$$\xi^{(k)} = \frac{z - (z^{(k-1)} + h^{(k)})}{h^{(k)}} \quad (k = 1, \dots, N) \quad (27)$$

where $z^{(0)} = -h$, $z^{(k)} = z^{(k-1)} + 2h^{(k)}$, and $z^{(N)} = h$. For a linear variation of the zigzag function across the thickness of every layer, with $\phi^{(k)} = u^{(k-1)}$ and $\phi^{(k)} = u^{(k)}$ for $\xi^{(k)} = -1$ and $\xi^{(k)} = 1$, respectively, the zigzag function used in Eqs. (1) is given by

$$\phi^{(k)} \equiv \frac{1}{2}(1 - \xi^{(k)}) u^{(k-1)} + \frac{1}{2}(1 + \xi^{(k)}) u^{(k)} \quad (28)$$

where $u^{(0)} = u^{(N)} = 0$. The above form of $\phi^{(k)}$ gives rise to a piecewise constant function $\beta^{(k)}$ ($\beta^{(k)} \equiv \phi_{,z}^{(k)}$) that may be expressed in terms of the layer-interface displacements as

$$\beta^{(k)} = \frac{u^{(k)} - u^{(k-1)}}{2h^{(k)}} \quad (29)$$

With this expression and the prescribed conditions $u^{(0)} = u^{(N)} = 0$, it is seen that the function $\beta^{(k)}$ has a particularly useful property that is true regardless of the layer material properties and thicknesses; that is,

$$\int_A \beta^{(k)} dA \equiv \frac{A}{2h} \sum_{k=1, N} 2h^{(k)} \beta^{(k)} = \frac{A}{2h} (u^{(N)} - u^{(0)}) = 0 \quad (30)$$

The usefulness of Eq. (30) is seen by integrating Eq. (5) over the beam cross-section. Performing this process and then recognizing the above $\beta^{(k)}$ property, gives

$$\gamma = \frac{1}{A} \int_A \gamma_{xz}^{(k)} dA \quad (31)$$

This equation verifies that $\gamma(x)$ is in fact the shear angle of the TBT and represents an average shear strain of the cross-section. Another useful application of Eq. (30) is found by multiplying both sides of Eq. (5) by $\beta^{(k)}$, and then integrating over the cross-sectional area. This process reveals that the function $\psi(x)$ is a weighted-average shear strain quantity given by

$$\psi = \frac{1}{\int_A (\beta^{(k)})^2 dA} \int_A \beta^{(k)} \gamma_{xz}^{(k)} dA \quad (32)$$

At this stage in the analysis, the layer-interface displacement, $u^{(k)}$, are yet unknown. Recall that in the zigzag models of Di Sciuva and Averill, the zigzag function was defined by prescribing the layer-interface displacements to be zero-valued for a specified layer, and by enforcing continuity of the transverse shear stresses at each layer interface. In the present study, instead of prescribing the layer-interface displacements to be zero-valued for a specified layer, the conditions $u^{(0)} = u^{(N)} = 0$ have been used. This approach allows a physically attractive partitioning of the TBT and zigzag kinematics, without introducing a bias in the kinematic equations.

In the manner of both the Di Sciuva and Averill schemes, the new refined zigzag model enforces interfacial continuity of the first term, associated with the $\gamma(x)$ variable, in the expression for the transverse shear stresses given by Eq. (6). Applying this process yields the conditions

$$G_{xz}^{(k)} (1 + \beta^{(k)}) = G_{xz}^{(k+1)} (1 + \beta^{(k+1)}) \quad (33)$$

for $k = 1, \dots, N - 1$. Thus, Eqs. (33) effectively establish a beam material constant defined by

$$G \equiv G_{xz}^{(k)} (1 + \beta^{(k)}) \quad (\text{constant}) \quad (34a)$$

Whereas this constraint strategy is fully consistent with the shear-stress continuity constraints developed by Di Sciuva, Eqs. (9) and (10), in the present setting because of an additional kinematic variable η , the conditions (33) do not enforce the interface shear-stress continuity. Furthermore, in contrast to Averill's penalty formulation, which enforces $\eta \rightarrow 0$ (Eq. (18)) and thus achieves shear-stress continuity in a limiting sense, the present refined zigzag model does not seek nor enforce continuity of the transverse shear stresses along the layer interfaces.

Obtaining $\beta^{(k)}$ from Eq. (34a),

$$\beta^{(k)} = G / G_{xz}^{(k)} - 1 \quad (34b)$$

and then invoking Eq. (30), i.e., integrating Eq. (34b) across the beam cross-section, gives rise to the expression for G in terms of the shear modulus and thickness of every layer. The resulting expression is

$$G = \left(\frac{1}{A} \int_A \frac{dA}{G_{xz}^{(k)}} \right)^{-1} \equiv h \left(\sum_{k=1, N} \frac{h^{(k)}}{G_{xz}^{(k)}} \right)^{-1} \quad (35)$$

Then, a recursion relation for the layer-interface displacements is found by substituting Eq. (34b) into Eq. (29) and accounting for Eq. (35); that is,

$$u^{(k)} = u^{(k-1)} + 2h^{(k)} \left(\frac{h}{G_{xz}^{(k)} \sum_{k=1, N} \frac{h^{(k)}}{G_{xz}^{(k)}}} - 1 \right); \quad (u^{(0)} = u^{(N)} = 0; \quad k = 1, \dots, N) \quad (36)$$

By substituting Eq. (34b) into Eq. (5), and using Eq. (4), the transverse shear strains may be conveniently expressed in terms of the constant and piecewise-constant components according to

$$\gamma_{xz}^{(k)} = \eta + \frac{G}{G_{xz}^{(k)}} \psi \quad (37)$$

Similarly, invoking Hooke's relations, Eqs. (3), the transverse shear stresses may be expressed as

$$\tau_{xz}^{(k)} = G \psi + G_{xz}^{(k)} \eta \equiv G \gamma + (G_{xz}^{(k)} - G) \eta \quad (38)$$

An alternative procedure that determines the same $\phi^{(k)}$ function as the one just presented can be developed from the energy minimization point of view and is summarized in Appendix C.

3.2 Constant stress requirement and penalization issues

The key issues concerning the validity and theoretical difficulties of the Di Sciuva and Averill zigzag models can now be clarified from the insight provided by the new, refined zigzag model. First, recall that in the Di Sciuva [7] and Averill [14] models, enforcing continuity of the transverse shear stresses across a cross-section, whether explicitly or as a limiting condition, results in an erroneous constant value for the transverse shear stress in a layer that does not depend on the corresponding shear moduli. This representation of the transverse shear stresses is generally a poor approximation of the actual transverse shear stresses present in a beam with a heterogeneous cross-section. Moreover, their approach produced a physical anomaly for a clamped boundary condition. The new zigzag model and the results of the present study reveal that the anomalies associated with the Di Sciuva and Averill models arise because the stress continuity constraints are fundamentally inconsistent with the kinematic freedom inherent in the lower-order kinematic approximations of the underlying beam theory. Naturally, higher-order approximations, such as the cubic zigzag model in [12], may provide the kinematic freedom required for consistent, continuous, non-constant transverse shear stresses.

The second issue that was clarified during the present study is the penalty enforcement, in Averill's model, which also produced a theoretical anomaly for a clamped boundary condition. The difficulty with this particular boundary condition was resolved unsatisfactorily in [14]. During the course of the present study, it was found that the penalization issue associated with the η function can be properly resolved at the constitutive-equation level, as opposed to adding an ad hoc penalty functional to the variational principle, as in [14]. In particular, a dimensionless penalty factor, λ_0 , can be introduced into the constitutive equation for the transverse shear stresses as follows

$$\tau_{xz(\lambda)}^{(k)} \equiv G \gamma + \lambda_0 (G_{xz}^{(k)} - G) \eta \quad (39)$$

where, for the special case $\lambda_0 = 1$, Eq. (39) reverts back to Eq. (38), which is the expression for the transverse shear stresses used in the refined zigzag model (although, for demonstration purposes, a few numerical results have been carried out with a large value of λ_0 and demonstrated in Section 5). The transverse shear strain energy associated with Eq. (39) is given by

$$U_{(\lambda)}^{shear} \equiv \frac{1}{2} \int_{x_a}^{x_b} \int_A \tau_{xz(\lambda)}^{(k)} \gamma_{xz}^{(k)} dA dx = \frac{GA}{2} \int_{x_a}^{x_b} \gamma^2 dx + \frac{\lambda}{2} \int_{x_a}^{x_b} \eta^2 dx \quad (40)$$

where λ denotes a penalty parameter (units of force) defined as

$$\lambda \equiv \lambda_0 \int_A G_{xz}^{(k)} (\beta^{(k)})^2 dA = \lambda_0 \left(\int_A G_{xz}^{(k)} dA - GA \right) \quad (41)$$

The first term in the shear strain energy has the same exact form as the shear strain energy of TBT, for a homogeneous beam, provided G is the beam's shear modulus. The second term is associated with the penalty parameter, λ . This second term appears naturally as a consequence of the modified constitutive relations and is amenable to physical interpretation. For homogeneous cross-sections, λ vanishes because $\beta^{(k)} = 0$ and G reduces to the beam's shear modulus. This approach is significantly different from Averill's penalization approach, where a similar penalty term is added to the strain energy *a posteriori*. The inclusion of the penalty factor λ_0 in Eq. (41), under the condition $\lambda_0 \rightarrow \infty$, allows for the limiting condition in Averill's model, given by Eq. (18), to be fulfilled. Also, note that the coupling term $\gamma \eta$ vanishes from the shear energy because of the intrinsic property of the new, refined zigzag function given by Eq. (30).

The fully consistent form of the present zigzag model is given by $\lambda_0 = 1$ in which Averill's limiting condition, Eq. (18), is not enforced. As a result, using $\lambda_0 = 1$ yields transverse shear stresses and strains that are piecewise constant across the laminated-beam cross-section and no anomalies are present for a clamped boundary condition. In addition, the same basic conclusions may be reached for any arbitrary value of λ_0 , including very large values. In this case, $\eta = O(\lambda^{-1})$, where O denotes the order of the quantity in parenthesis. Even for values of $\lambda_0 \rightarrow \infty$, the second term of the shear stress expression in Eq. (39) does not vanish and is $O(G - G_{xz}^{(k)})$.

3.3 Virtual work principle, equilibrium equations, and boundary conditions

For the beam defined in Figure 1, the virtual work principle (VWP) may be expressed as

$$\begin{aligned} & \int_{x_a}^{x_b} \int_A \left(\sigma_x^{(k)} \delta \varepsilon_x^{(k)} + \tau_{xz(\lambda)}^{(k)} \delta \gamma_{xz}^{(k)} \right) dA dx - \int_{x_a}^{x_b} q \delta w dx \\ & + \int_A \left[T_{xa} \delta u_x^{(k)}(x_a, z) + T_{za} \delta w(x_a) \right] dA - \int_A \left[T_{xb} \delta u_x^{(k)}(x_b, z) + T_{zb} \delta w(x_b) \right] dA = 0 \end{aligned} \quad (42)$$

where δ denotes the variational operator. Performing the cross-sectional integration and variation by parts, results in the following equilibrium equations

$$\begin{aligned}
N_{x,x} &= 0 \\
M_{x,x} - V_x &= 0 \\
V_{x,x} + q &= 0 \\
M_{\phi,x} - V_\phi &= 0
\end{aligned} \tag{43}$$

and a consistent set of boundary conditions

$$\begin{aligned}
&\text{either } u(x_\alpha) = \bar{u}_\alpha \quad \text{or} \quad N_x(x_\alpha) = \bar{N}_{x\alpha} \\
&\text{either } \theta(x_\alpha) = \bar{\theta}_\alpha \quad \text{or} \quad M_x(x_\alpha) = \bar{M}_{x\alpha} \\
&\text{either } w(x_\alpha) = \bar{w}_\alpha \quad \text{or} \quad V_x(x_\alpha) = \bar{V}_{x\alpha} \\
&\text{either } \psi(x_\alpha) = \bar{\psi}_\alpha \quad \text{or} \quad M_\phi(x_\alpha) = \bar{M}_{\phi\alpha}
\end{aligned} \tag{44}$$

where $\alpha=a,b$ and the bar-superscripted symbols denote the prescribed displacements and stress resultants.

The first three equilibrium equations in Eqs. (43) are the same as those in the conventional Euler-Bernoulli Beam Theory and Timoshenko Beam Theory. The fourth equation describes the moment-shear equilibrium associated with the contribution of the zigzag function to the bending moment and shear force. The stress resultants appearing in these equations are given by

$$(N_x, M_x, M_\phi, V_x, V_\phi) \equiv \int_A (\sigma_x^{(k)}, z\sigma_x^{(k)}, \phi^{(k)}\sigma_x^{(k)}, \tau_{xz}^{(k)}, \beta^{(k)}\tau_{xz}^{(k)}) dA \tag{45}$$

$$(\bar{N}_{x\alpha}, \bar{M}_{x\alpha}, \bar{M}_{\phi\alpha}, \bar{V}_{x\alpha}) \equiv \int_A (T_{x\alpha}, zT_{x\alpha}, \phi^{(k)}T_{x\alpha}, T_{z\alpha}) dA \tag{46}$$

where N_x , M_x , and V_x are respectively the conventional axial force, bending moment, and shear force.

The symbols M_ϕ and V_ϕ are the bending moment and shear force associated with the contribution of the zigzag function. The corresponding beam constitutive relations are obtained by substituting the strain-displacement relations into the constitutive relations, given by Eqs. (3), and then substituting the resulting expression into the stress resultants defined by Eqs. (45) and integrating over the cross-sectional area. The resulting constitutive relations of the new zigzag beam theory are

$$\begin{Bmatrix} N_x \\ M_x \\ M_\phi \end{Bmatrix} = \begin{bmatrix} A_1 & B_2 & B_3 \\ B_2 & D_{11} & D_{12} \\ B_3 & D_{12} & D_{22} \end{bmatrix} \begin{Bmatrix} u_x \\ \theta_x \\ \psi_x \end{Bmatrix} \tag{47}$$

$$\begin{Bmatrix} V_x \\ V_\phi \end{Bmatrix} = \begin{bmatrix} Q_{11}^2 & Q_{12}^2 \\ Q_{12}^2 & Q_{22}^2 \end{bmatrix} \begin{Bmatrix} \theta + w_{,x} \\ \psi \end{Bmatrix} \tag{48}$$

where the stiffness coefficients are defined in Appendix A.

Substituting the expressions for the stress resultants in Eqs. (47) and (48) into Eqs. (43) yields the equilibrium equations in terms of the primary kinematic variables of the theory. This eighth-order system of ordinary differential equations, with constant coefficients, is given by

$$\begin{aligned}
 A_{11}u_{,xx} + B_{12}\theta_{,xx} + B_{13}\psi_{,xx} &= 0 \\
 Q_{11}^i(w_{,xx} + \theta_{,x}) + Q_{12}^i\psi_{,x} &= -q(x) \\
 B_{12}u_{,xx} + D_{11}\theta_{,xx} + D_{12}\psi_{,xx} - Q_{11}^i(w_{,x} + \theta) - Q_{12}^i\psi &= 0 \\
 B_{13}u_{,xx} + D_{12}\theta_{,xx} + D_{22}\psi_{,xx} - Q_{12}^i(w_{,x} + \theta) - Q_{22}^i\psi &= 0
 \end{aligned} \tag{49}$$

Solution of the corresponding boundary-value problem involves integration of the four equilibrium equations, given by Eqs. (49), subject to the boundary conditions given by Eqs. (44). For problems with forces specified at the ends of a beam, the constitutive relations given by Eqs. (47) and (48) are used to express the force boundary conditions in terms of the primary kinematic variables.

4. Examples and Analytic Solutions

The predictive capability of the new, refined zigzag beam theory is demonstrated for two beam examples that provide a challenge to the theory for certain laminate constructions and beam-slenderness ratios. The first example is a simply supported beam of length L that is subjected to the sinusoidal transverse line load $q(x) = q_0 \sin(\pi x/L)$, as shown in Figure 5.

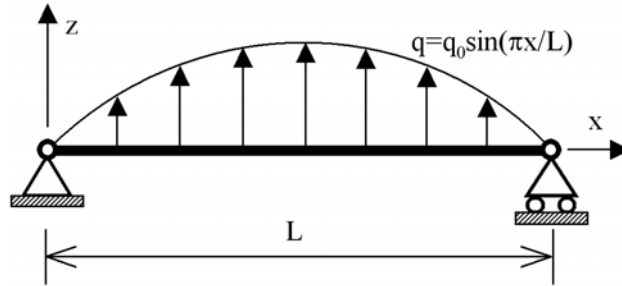


Figure 5. Simply supported beam subjected to a sinusoidal transverse line load.

The boundary conditions at the ends $x = 0$ and $x = L$ of the beam are

$$w = N_x = M_x = M_\phi = 0 \tag{50}$$

The following trigonometric expressions for the four kinematic variables

$$\begin{aligned}
w(x) &= w_0 \sin(\pi x/L), \\
(u(x), \theta(x), \psi(x)) &= (u_0, \theta_0, \psi_0) \cos(\pi x/L)
\end{aligned} \tag{51}$$

satisfy the above boundary conditions exactly. The amplitudes w_0 , u_0 , θ_0 , and ψ_0 are determined uniquely, and the boundary-value problem is solved, by substituting Eqs. (51) into the equilibrium equations, Eqs. (49), and then solving the resulting system of four linear algebraic equations.

The second example presented herein is a cantilevered beam of length L that is subjected to a transverse load F at the free end, as shown in Figure 6. The boundary conditions are given by

$$\begin{aligned}
x = 0: \quad u = w = \theta = \psi = 0 \\
x = L: \quad N_x = M_x = M_\phi = 0, \quad V_x = F
\end{aligned} \tag{52}$$

Because $q(x) = 0$ for this problem, the equilibrium equations, Eqs. (49), can be rewritten in the more convenient form

$$\begin{aligned}
C_1 \psi_{,xxx} + C_2 \psi_{,x} &= 0 \\
\theta_{,xx} &= -C_3 \psi_{,xx} + \frac{C_2}{D_{11}^*} \psi \\
w_{,x} &= -\theta - C_4 \psi + C_5 \theta_{,xx} + C_6 \psi_{,xx} \\
u_{,xx} &= -C_7 \theta_{,xx} - C_8 \psi_{,xx}
\end{aligned} \tag{53}$$

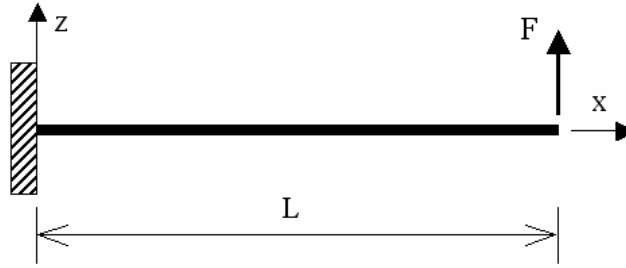


Figure 6. Cantilevered beam subjected to a transverse tip load.

The coefficients, which are dependent on the material properties, are presented in Appendix B. Integrating these equations by using the standard technique for ordinary differential equations yields the following expressions for the kinematic variables

$$\psi(x) = a_1 \cosh(Rx) + a_2 \sinh(Rx) + a_3,$$

$$\begin{aligned}
\theta(x) &= \left(-C_3 + \frac{C_2}{R^2 D_{11}^*} \right) (a_1 \cosh(Rx) + a_2 \sinh(Rx)) + \frac{C_2 a_3}{2 D_{11}^*} x^2 + a_4 x + a_5, \\
u(x) &= \left(-C_8 + C_3 C_7 - \frac{C_2 C_7}{R^2 D_{11}^*} \right) (a_1 \cosh(Rx) + a_2 \sinh(Rx)) - \frac{C_2 C_7 a_3}{2 D_{11}^*} x^2 + a_6 x + a_7, \quad (54) \\
w(x) &= \left[\frac{C_3}{R} - \frac{C_2}{R^3 D_{11}^*} + \frac{1}{R} \left(\frac{C_2 C_5}{D_{11}^*} - C_4 \right) + R(C_6 - C_3 C_5) \right] (a_1 \sinh(Rx) + a_2 \cosh(Rx)) \\
&\quad - \frac{C_2 a_3}{6 D_{11}^*} x^3 - \frac{a_4}{2} x^2 + \left[\left(\frac{C_2 C_5}{D_{11}^*} - C_4 \right) a_3 - a_5 \right] x + a_8
\end{aligned}$$

where the a_i ($i = 1, \dots, 8$) unknown constants are determined from the boundary conditions stated by Eqs. (52).

5. Results and Discussion

Results are presented in this section for the two beam examples previously described. The results include comparisons of those obtained from the new zigzag theory to those obtained from the TBT, Di Sciuva's and Averill's zigzag models, exact elasticity solutions, and high-fidelity finite element solutions. A thick, three-layer beam is considered for all problems, with total depth $2h = 2$ [cm] and length $L = 10$ [cm]. The span-to-depth ratio is $L/2h = 5$ and each beam has a rectangular cross-section. The mechanical properties of six layer materials that were used to generate results are presented in Table 1. The major principal axis of each material is aligned parallel to the beam axis. Three unidirectional laminate stacking sequences that were considered are presented in Table 2.

Table 1. Mechanical properties of the beam layer materials.

Material type	$E_x^{(k)}$ [GPa] (Young's modulus)	$G_{xz}^{(k)}$ [GPa] (Shear modulus)
a	73.0	29.2
b	21.9	8.76
c	3.65	1.46
d	0.73	0.292
e	0.219	0.088
f	0.073	0.029

Table 2. Stacking sequences of three-layer beams
(layer sequence is in the positive z direction).

Laminate	Thicknesses [cm]	Materials
A	(0.20/1.60/0.20)	(a/f/b)
B	(0.66/0.66/0.66)	(b/e/b)
C	(0.66/0.66/0.66)	(d/a/c)

The layer thicknesses are presented in the form $(2h^{(1)}, 2h^{(2)}, 2h^{(3)})$ and the first layer in each laminate starts at $z = -h$. Similarly, the material composition of each layer is presented in the form $(M^{(1)}, M^{(2)}, M^{(3)})$, where “ M ” denotes the material type. The first stacking sequence, designated as Laminate A in Table 2, is an asymmetrically laminated sandwich construction with a core that is eight times thicker than the face sheets. In addition, the core is made of material “f” and is three orders of magnitude more compliant than the bottom face sheet, which is made of material “a.” Moreover, the top face sheet has the same thickness as the bottom face sheet, but is about three times more compliant. The extreme heterogeneity of this stacking sequence results in beam examples that are very challenging for the beam theories considered herein to model adequately. Laminate B has three equal-thickness layers, with the outer layers having the same stiffness properties, and where the middle layer is two orders of magnitude more compliant than the outer layers. Moreover, this laminate is symmetric with respect to the mid-depth reference axis. Laminate C also has three equal-thickness layers; however, unlike Laminate B, here the middle layer is two orders of magnitude stiffer compared to the bottom layer. Also note that this laminate does not possess material symmetry with respect to the mid-depth reference axis since the top layer, made of material “c”, is five times stiffer than the bottom layer, made of material “d”. These three distinctly different laminates thus constitute a diverse set of practical and challenging material configurations that represent realistic bounds in industrial applications.

Results for simply supported beams made from Laminates A and C are presented in Figures 7-12, and results for cantilevered beams made from Laminates A and B are presented in Figures 13-26. Several curves are presented in each figure, as indicated by their figure legends. For conciseness, the following legend captions are used. The legend caption “Exact” refers to the exact elasticity solution for a simply supported plate in a state of cylindrical bending that was presented by Pagano [19]. Although this solution is for a plate, the results are also applicable to beams. The legend caption “FEM/NASTRAN” refers to a high-fidelity, two-dimensional FEM solution obtained with the MSC/NASTRAN[®] code [21]. The details of this solution are described in Appendix D. The legend caption “TBT” refers to the exact solutions obtained from the Timoshenko Beam Theory. For these solutions, the standard shear correction factor $k^2 = 5/6$ was used throughout, which is appropriate for homogeneous beam with a rectangular cross-section. Note that various approaches have been proposed for determining shear correction factors for laminated beams that often provide more accurate transverse deflection results. The choice of a shear correction to be used with TBT, however, does not influence the prediction of the axial and transverse shear stresses. The legend caption “Zigzag (D, A)” refers to exact solutions obtained with the Di Sciuva [7] and Averill [14] zigzag models, for the cases when virtually identical results are produced. The caption “Zigzag (R)” indicates solutions obtained using the refined zigzag theory with $\lambda_0=1$. Similarly,

“Zigzag (R($\lambda_0=10^6$))” refers to solutions obtained using the refined zigzag theory with $\lambda_0=10^6$. The caption “Zigzag (All)” refers to nearly identical solutions obtained by all three zigzag models presented herein. Lastly, the legend caption “Integrated” refers to the transverse shear stresses obtained by integrating the equilibrium equation $\sigma_{x,x}^{(k)} + \tau_{xz,z}^{(k)} = 0$, in which $\sigma_x^{(k)}$ represents the axial stress determined from the refined zigzag theory ($\lambda_0=1$). This commonly employed transverse shear stress-recovery method has been shown to produce accurate shear stresses $\tau_{xz}^{(k)}$ that are in close agreement with the corresponding results obtained from the high-fidelity finite element model described in Appendix D.

In Figures 7-26, the axial and transverse coordinates are normalized as $(\tilde{x}, \tilde{z}) \equiv (x/L, z/h)$. Similarly, for the simply supported beams, the following dimensionless solution variables are used

$$\left(\tilde{u}_x^{(k)}, \tilde{u}_z^{(k)}\right) \equiv \frac{\pi^4 D_{11}}{10 q_0 L^4} \left(u_x^{(k)}, u_z^{(k)}\right), \quad \left(\tilde{\sigma}_x^{(k)}, \tilde{\tau}_{xz}^{(k)}\right) \equiv \frac{2h A \pi^2}{q_0 L^2} \left(\sigma_x^{(k)}, \tau_{xz}^{(k)}\right) \quad (55)$$

For the cantilevered beams, the dimensionless solution variables are given by the expressions

$$\left(\tilde{u}_x^{(k)}, \tilde{u}_z^{(k)}, \tilde{w}\right) \equiv \frac{D_{11}}{10 F L^3} \left(u_x^{(k)}, u_z^{(k)}, w\right), \quad \left(\tilde{\sigma}_x^{(k)}, \tilde{\tau}_{xz}^{(k)}\right) \equiv \frac{2h A}{F L} \left(\sigma_x^{(k)}, \tau_{xz}^{(k)}\right), \quad (56)$$

$$\tilde{V}_x \equiv \frac{1}{F} \int_A \tau_{xz}^{(k)} dA$$

5.1 Results for Simply Supported Beams

Normalized axial displacements, transverse displacements, and transverse shear stress distributions are presented in Figures 7-9, respectively, for the simply supported beam made from Laminate A – a three-layer sandwich with a very thick, compliant core. Three curves are shown in Figures 7 and 9 and two curves are shown in Figure 8. The solid and dashed black curves correspond to results from the exact elasticity solution and all three zigzag models presented herein, respectively. The finely dashed gray line corresponds to results from the TBT. The abscissa in Figure 8 is scaled to exaggerate the difference in the results obtained from the exact elasticity solution and the three zigzag models. As a result, the transverse deflection obtained from the TBT, $\tilde{u}_z(L/2) = 0.164$, is not shown.

The results in Figures 7-9 show that modeling the deformations of Laminate A is a particularly challenging problem for any structural theory. The beam is relatively deep ($L/2h = 5$) and has a high degree of heterogeneity typical of sandwich construction: a highly compliant thick layer bounded by two relatively stiff, thin face sheets. For this problem, Timoshenko theory under predicts the deflection by a factor of about 15 (Figure 8). All zigzag theories produce comparable displacement and stress results that correlate well with the exact solutions. As seen from Figure 9, only slight differences are observed in the shear stress as predicted by the Di Sciuva, Averil and refined zigzag theories, its distribution being respectively constant and piece-wise constant. Contrasted with the zigzag results, Timoshenko’s shear stress is substantially under estimated in the core and grossly over estimated in the face sheets.

Laminate C has three layers of equal thickness, with a very stiff inner layer (Figures 10-12). For this laminate, the TBT models the overall beam stiffness adequately and produces accurate displacement and

transverse shear stress predictions. As shown in Figure 11, the refined zigzag theory, when used with a large penalty factor, $\lambda_0=10^6$, produces a slightly lower deflection than in the $\lambda_0=1$ case, where the latter solution only slightly exceeds the exact value at $\tilde{z}=0$. Also note that the deflection solution corresponding to the $\lambda_0=10^6$ case is closely correlated with the Di Sciuva and Averill predictions that are somewhat stiffer than those of the refined theory with $\lambda_0=1$. As evidenced from Figure 12, the refined zigzag theory demonstrates a notable improvement in the transverse shear stress predictions over the other zigzag theories considered herein. This example clearly demonstrates that, even for the simply supported case, the other zigzag theories may produce rather inaccurate shear stresses, even when compared to those of the TBT. Moreover, the non penalized form ($\lambda_0=1$) of the refined zigzag theory produces slightly more flexible and accurate results than its penalized ($\lambda_0=10^6$) counterpart. For this reason, subsequent results for the refined zigzag theory are only demonstrated for the non penalized case ($\lambda_0=1$).

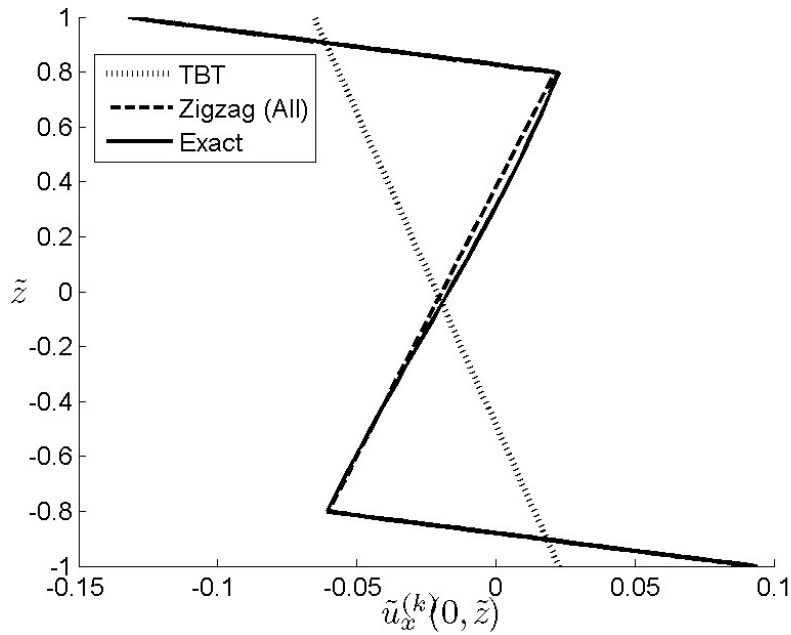


Figure 7. Normalized axial displacement at the left end of a simply supported beam with laminate A stacking sequence.

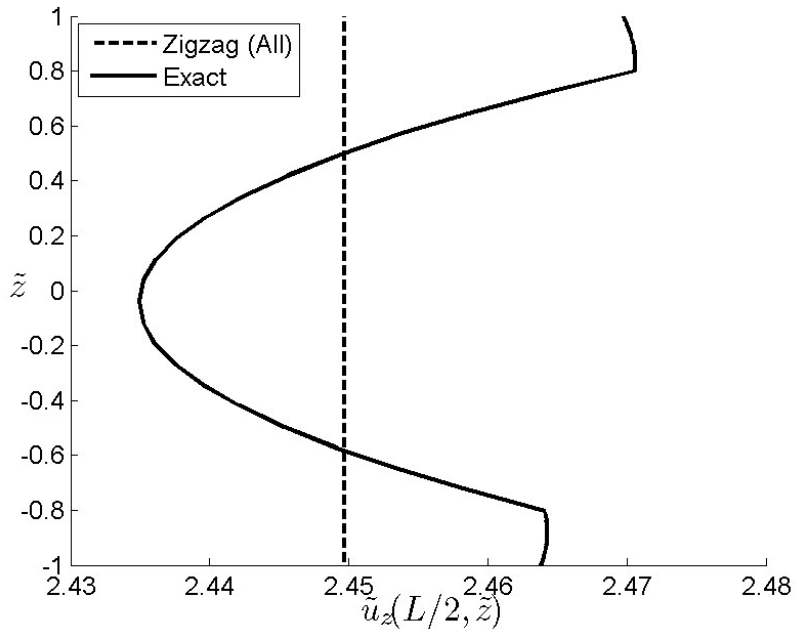


Figure 8. Normalized transverse mid-span displacement of simply supported beam with laminate A stacking sequence.

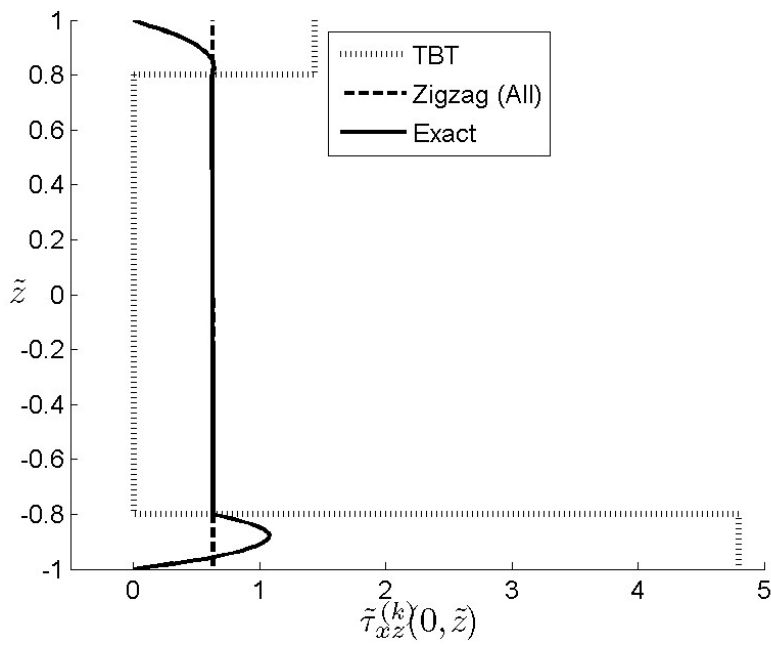


Figure 9. Normalized transverse shear stress at left end of simply supported beam with laminate A stacking sequence.

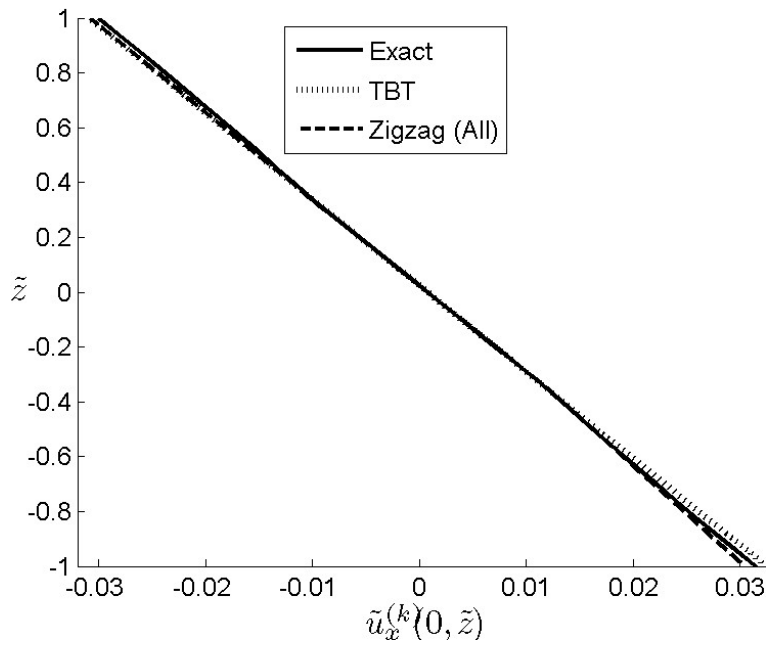


Figure 10. Normalized axial displacement at left end of simply supported beam with laminate C stacking sequence.

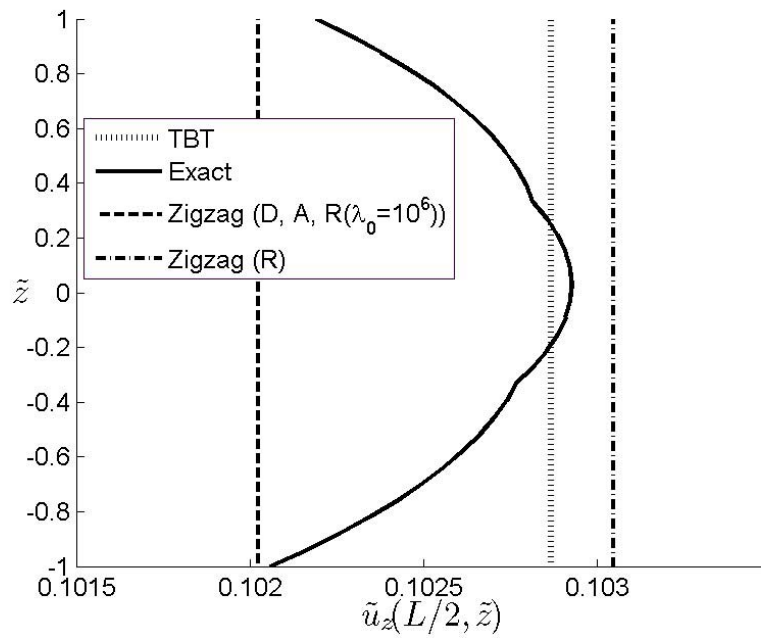


Figure 11. Normalized transverse displacement at mid-span of simply supported beam with laminate C stacking sequence.

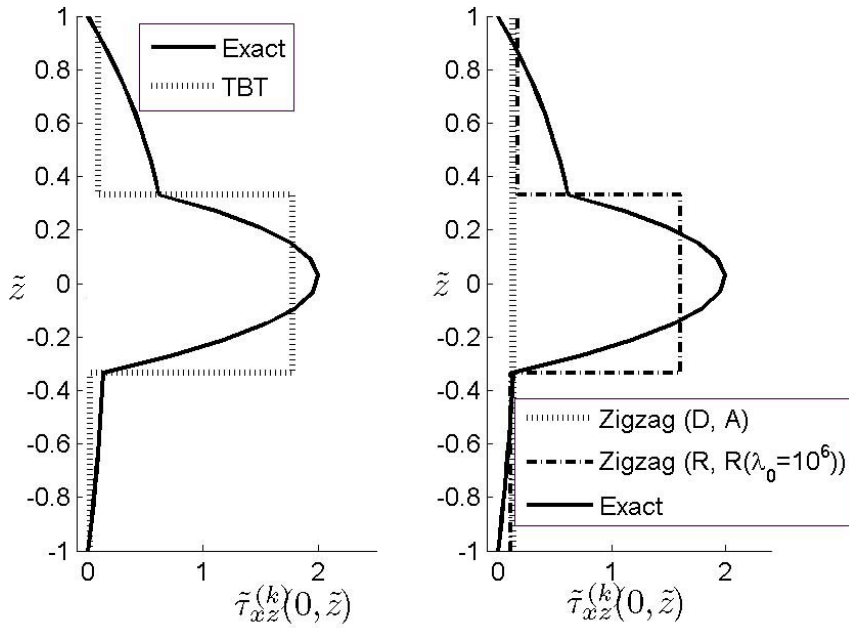


Figure 12. Normalized transverse shear stress at left end of simply supported beam with laminate C stacking sequence.

5.2 Results for Cantilevered Beams

In this section, results are examined for the cantilevered beam problem for Laminates A and B (Figures 13-26). The sandwich-type Laminate A is again a major challenge for the TBT, which over estimates the over all stiffness of the beam and under estimates the maximum deflection by over 80% and the maximum axial stress by over 50% (Figures 13 and 14). These results are in great contrast with those of the zigzag theories, which produce very accurate displacements and stresses.

Differences between the various zigzag solutions are observed by examining the through-the-depth distributions predicted for the displacements and stresses at various locations along the span, including the clamped end. The axial stress and displacement depicted in Figures 14-16 are accurately modeled by all three zigzag theories examined, exhibiting only minor quantitative differences. The good agreement is attributed to their built-in zigzag kinematics, giving rise to the requisite slope changes at the layer interfaces due to the layer differences in shear moduli.

Examination of the transverse shear stress predictions reveals specific differences in the capabilities of the beam theories examined. At the clamped end (Figures 17), the refined zigzag theory yields a non-vanishing stress, whereas the Di Sciuva and Averill zigzag theories predict an erroneous, zero shear stress. Away from the clamped end (Figures 18 and 19), the shear stress distributions also exhibit substantial differences. For this problem, the cross-sectional distribution of the shear stress changes significantly along the beam's span, as expressed by the shear stress obtained through the integration

procedure (highlighted in Section 5) and the refined zigzag theory. The Di Sciuva and Averill zigzag theories produce a shear stress that varies in magnitude with respect to the axial coordinate, while remaining constant across individual cross-sections. The shear stress of the refined zigzag theory also varies with respect to the axial coordinate; however, it is piece-wise constant across the cross-sections. In contrast, the shear stress of the TBT remains constant with respect to the axial coordinate and exhibits inferior accuracy across the beam’s cross-sections. Finally, the shear force distribution along the beam’s span (Figure 20) clearly illustrates the transverse-shear force anomaly inherent in the Di Sciuva and Averill zigzag theories. As shown in Figure 20, the Di Sciuva and Averill zigzag theories predict that the normalized shear force quantity, \tilde{V}_x , vanishes at the clamped end. Nearly halfway across the beam, an asymptotic value is achieved that over estimates the correct value by about 10%. Note, however, that a correct shear force distribution is obtained from Di Sciuva’s theory when it is calculated by taking the derivative of the bending moment. Both the TBT and the refined zigzag theory give rise to a correct, constant shear force over the entire span of the beam.

Laminate B has three equal-thickness layers and possesses a material symmetry with respect to the mid-depth reference axis. For this laminate, the solution obtained by the TBT is overly stiff, with the maximum deflection underestimated by about 50% (Figure 21). In contrast, results from the refined zigzag theory are consistently accurate. Specifically, the refined zigzag theory models the span-wise variation in the transverse shear stress distribution across each cross-section accurately (Figures 22-25). In Figure 26 are depicted the normalized shear force distributions, \tilde{V}_x , along the beam span. As in Figure 20, the key theoretical anomaly of Di Sciuva’s theory is manifested by \tilde{V}_x vanishing at the clamped end. It is noted once again that a correct shear force distribution corresponding to Di Sciuva’s theory is given by the derivative of the bending moment.

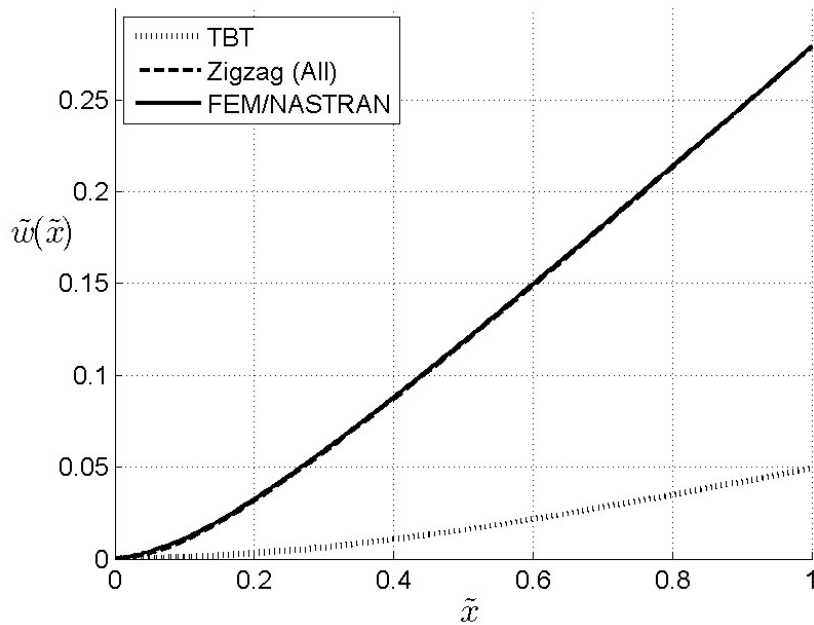


Figure 13. Normalized deflection of cantilevered beam with laminate A stacking sequence.

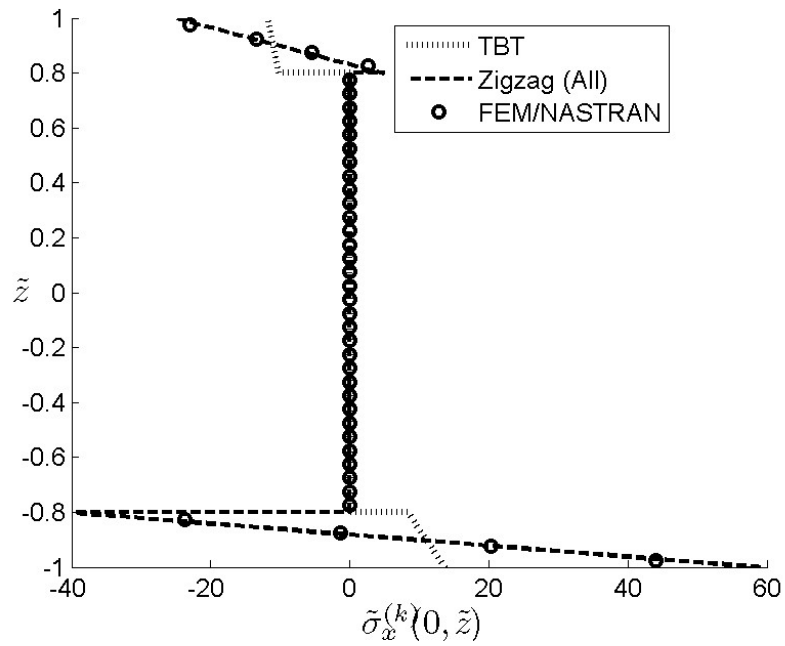


Figure 14. Normalized axial stress at the clamped end of cantilevered beam with laminate A stacking sequence.

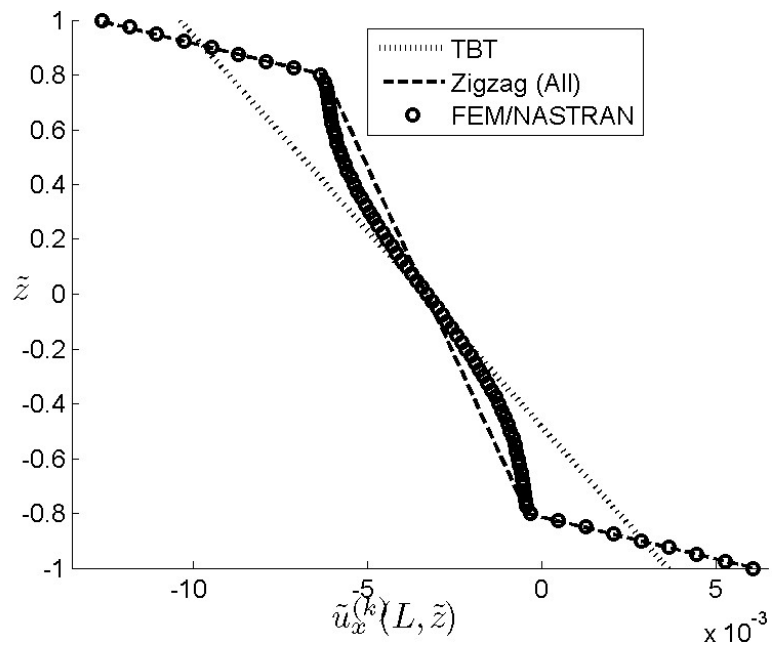


Figure 15. Normalized axial displacement at the free end of cantilevered beam with laminate A stacking sequence.

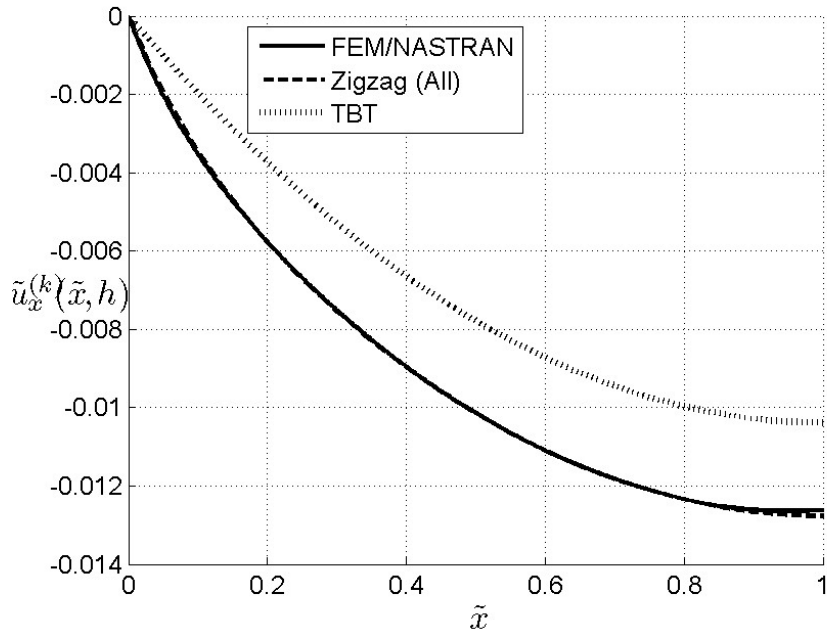


Figure 16. Normalized axial displacement along the top face of a cantilevered beam with laminate A stacking sequence.

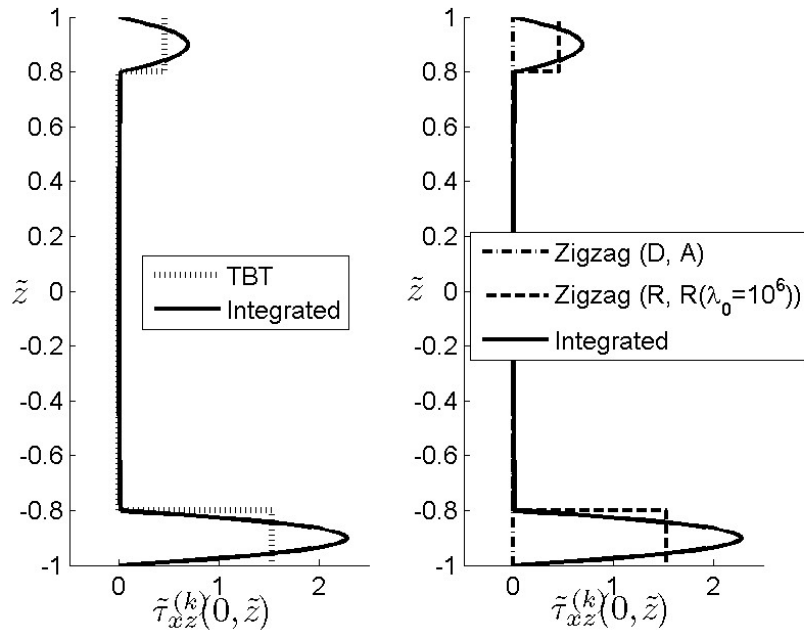


Figure 17. Normalized transverse shear stress at the clamped end of a cantilevered beam with laminate A stacking sequence.

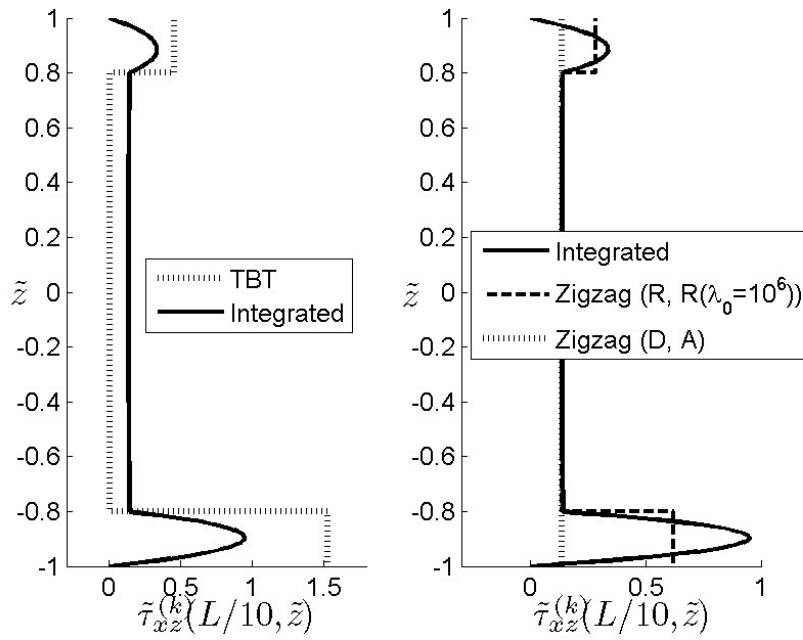


Figure 18. Normalized transverse shear stress at $x=L/10$ of a cantilevered beam with laminate A stacking sequence.

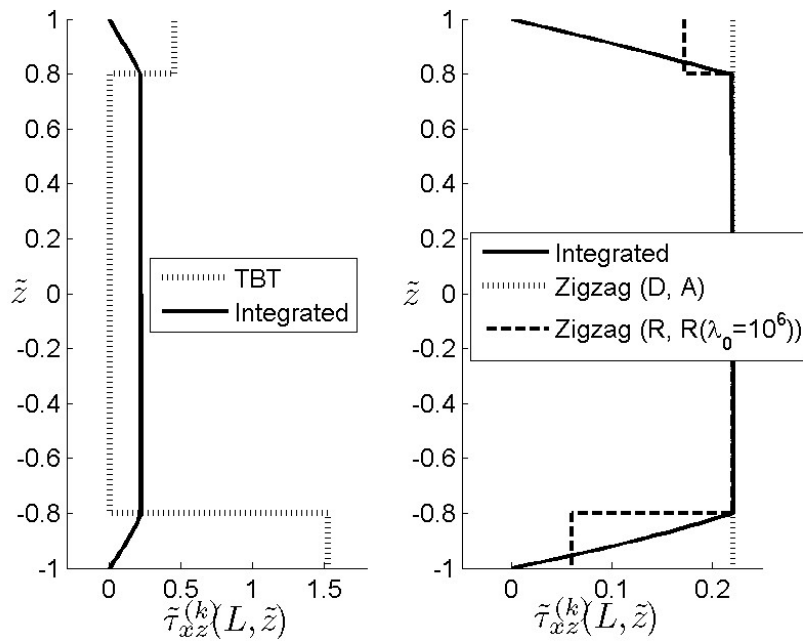


Figure 19. Normalized transverse shear stress at the free end of a cantilevered beam with laminate A stacking sequence.

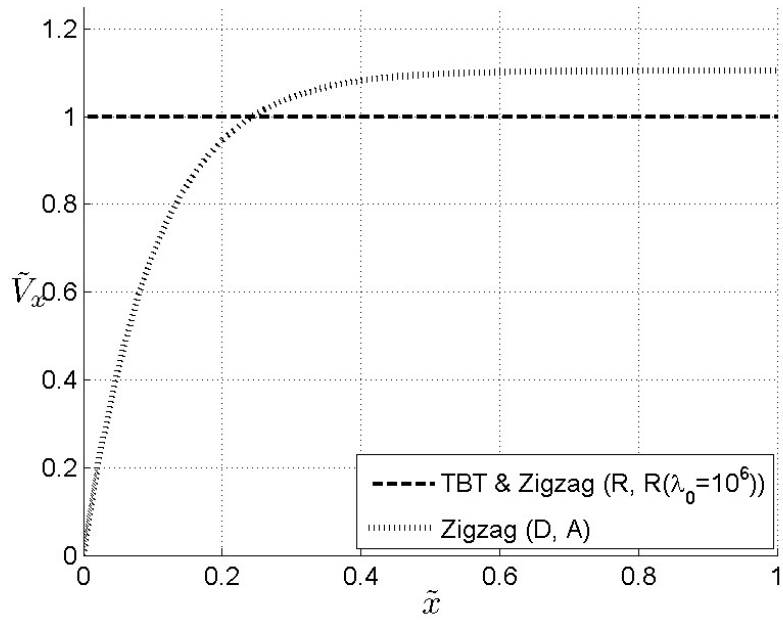


Figure 20. Normalized shear force along a cantilevered beam with laminate A stacking sequence.

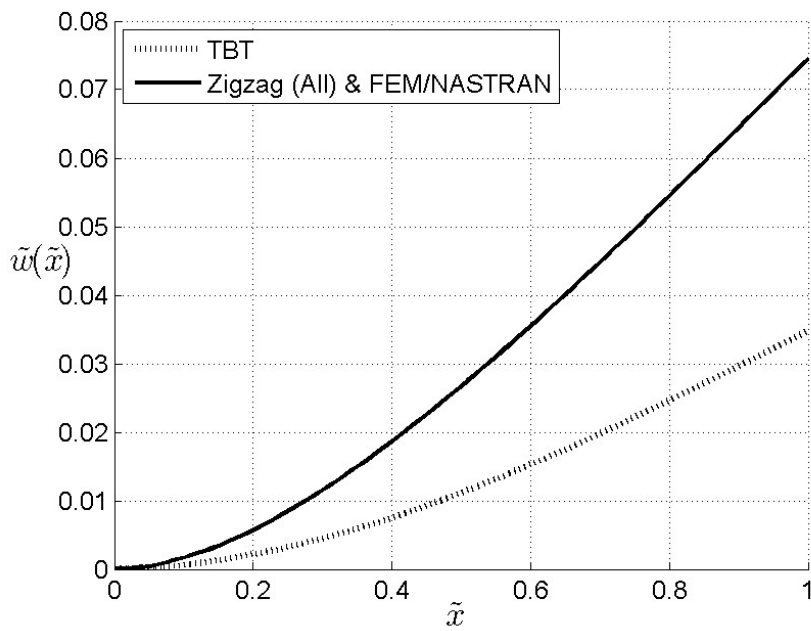


Figure 21. Normalized deflection along a cantilevered beam with laminate B stacking sequence.

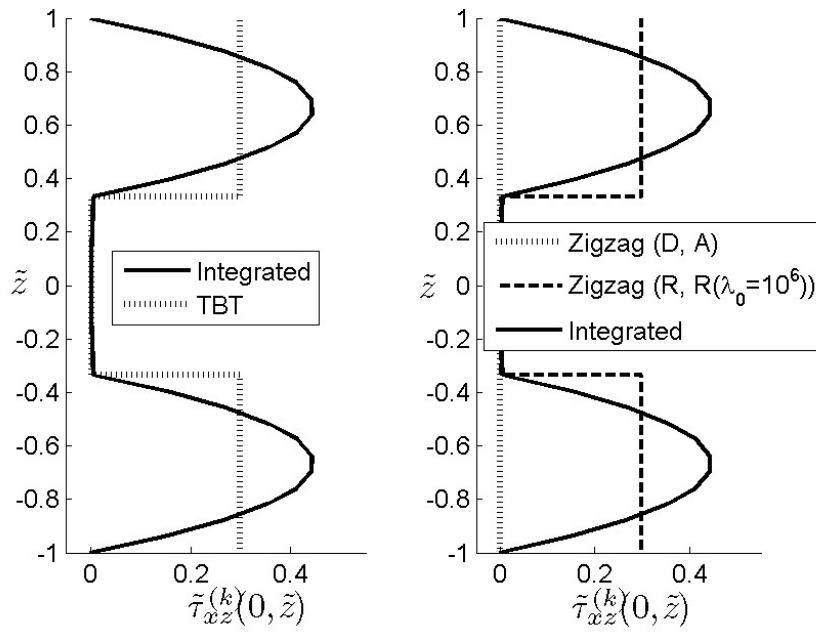


Figure 22. Normalized transverse shear stress at the clamped end of a cantilevered beam with laminate B stacking sequence.

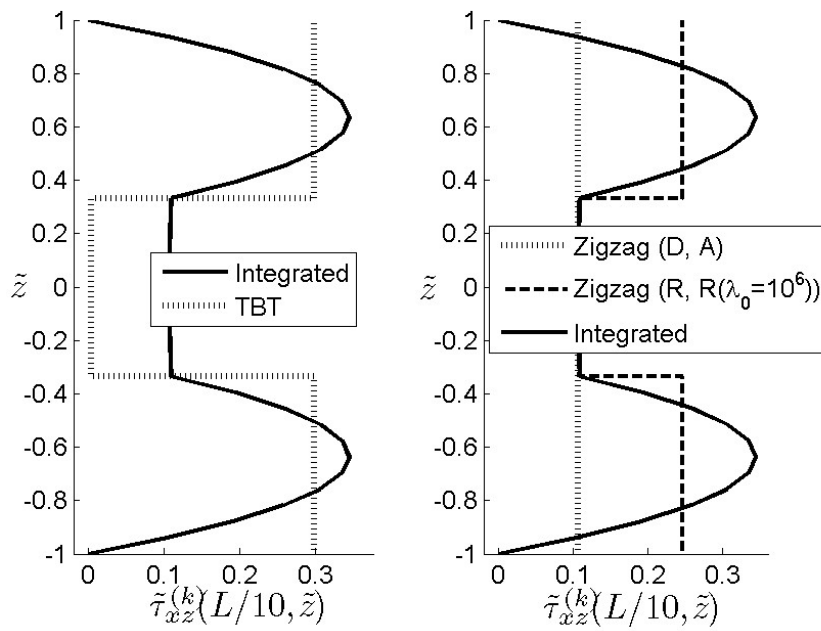


Figure 23. Normalized transverse shear stress at $x=L/10$ of a cantilevered beam with laminate B stacking sequence.

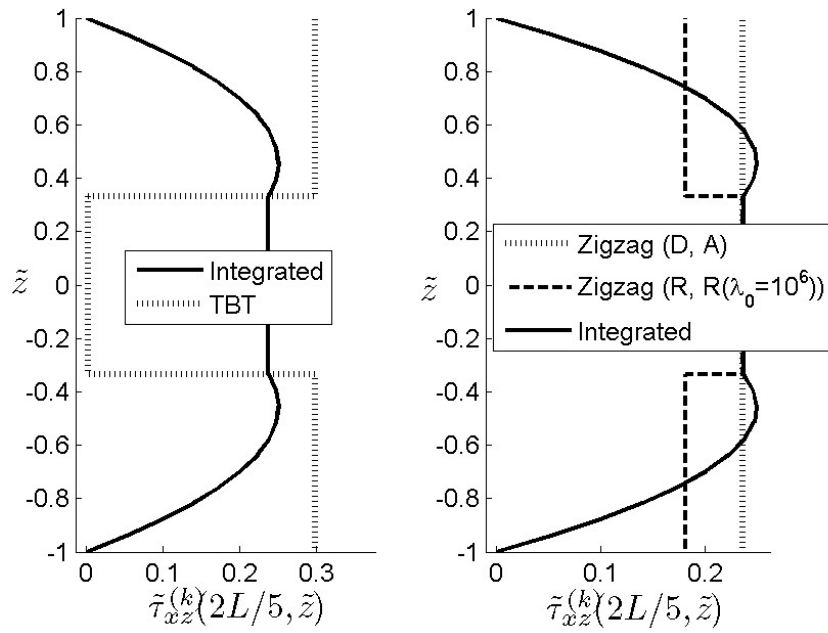


Figure 24. Normalized transverse shear stress at $x=2L/5$ of a cantilevered beam with laminate B stacking sequence.

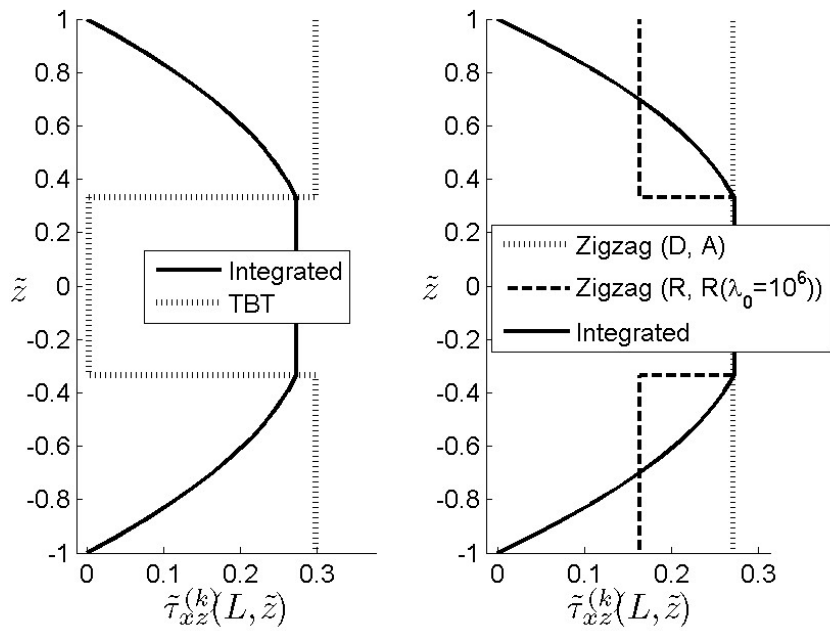


Figure 25. Normalized transverse shear stress at the free end of a cantilevered beam with laminate B stacking sequence.

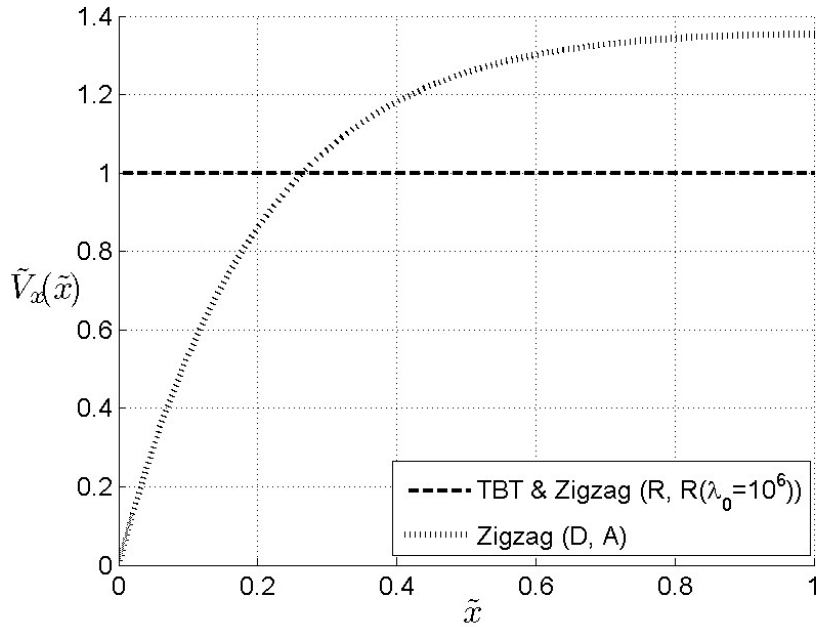


Figure 26. Normalized shear force along the span of a cantilevered beam with laminate B stacking sequence.

6. Conclusions

A new, refined “zigzag” theory for laminated-composite and sandwich beams that exhibit a high degree of transverse shear flexibility has been presented. The kinematic assumptions of this theory employ a novel piecewise continuous representation of the displacement field that is independent of the number of material layers, does not require enforcement of transverse-shear-stress continuity to yield accurate results, and that is zero-valued at the top and bottom surfaces of a beam. Additionally, the force equilibrium equations, boundary conditions, and strain-displacement relations are completely consistent, with respect to the virtual work principle, and a transverse-shear correction factor is not required. This new theory is better suited for engineering practice than previous theories because of its relative simplicity and its ability to model accurately the transverse shear and axial deformations of the individual layers in a physically realistic manner. Unlike other theories, meaningful axial and shear stresses are obtained directly from the constitutive equations, in a theoretically consistent manner, in this new theory. Moreover, the resultant transverse shear force acting at a beam cross-section can be obtained by integrating the corresponding transverse shear stress directly. These two physically attractive, fundamental properties are unique to this new theory. Similarly, this new theory is devoid of a major shortcoming of other similar theories; that is, the new theory enables accurate modeling of the clamped boundary condition.

Results have been presented for simply supported and clamped beams with highly heterogeneous material lay-ups and relatively small span-to-depth ratios. These results are for beam constructions that are extremely difficult for beam theories to model accurately. Comparisons with corresponding results obtained from exact two-dimensional elasticity analyses, high-fidelity finite element analyses, and other beam theories have also been presented. These comparisons show that the new, refined zigzag theory provides highly accurate predictions of displacements, stresses, and force resultants.

Finally, this new theory is amenable to the development of computationally efficient C^0 -continuous finite elements that can be implemented into general purpose codes used to design an important class of high-performance aerospace structures, and is readily extendable to theories for thick, highly heterogeneous plate and shell structures.

Acknowledgments

The first author would like to acknowledge the support for this work provided by the Floyd L. Thompson NASA Fellowship. The third author gratefully acknowledges NIA – National Institute of Aerospace (Hampton, VA) for inviting and hosting him as a Visiting Researcher in the framework of “2007 Visitor Program” and acknowledges Politecnico di Torino for supporting his research activity at NIA in the framework of “Young Researchers Program“ (2006 and 2007).

References

- [1] Timoshenko S., 1921: *On the correction for shear of differential equations for transverse vibrations of prismatic bars*. Philosophical Magazine Series, Vol. 41, pp. 744-746.
- [2] Liu D. and Li X., 1996: *An overall view of laminate theories based on displacement hypothesis*. Journal of Composite Materials, Vol. 30(14), pp. 1539-1561.
- [3] Ambartsumian S. A., 1964: *Theory of anisotropic shells*. NASA TTF-118.
- [4] Sun C. T. and Whitney J. M., 1973: *Theories for the dynamic response of laminated plates*. AIAA Journal, Vol. 11(2), pp. 178-183.
- [5] Di Sciuva M., 1987: *An improved shear-deformation theory for moderately thick multilayered anisotropic shells and plates*. ASME Journal of Applied Mechanics, Vol. 54, pp. 589-596.
- [6] Di Sciuva M., 1984: *A refinement of the transverse shear deformation theory for multilayered orthotropic plates*. Proceedings of 7th AIDAA National Congress, October 1983; also published in L'aerotecnica missili e spazio, Vol. 62, pp. 84-92.

- [7] Di Sciuva M., 1984: *A refined transverse shear deformation theory for multilayered anisotropic plates*. Atti Accademia delle Scienze di Torino, Vol. 118, pp. 279-295.
- [8] Di Sciuva M., 1986: *Bending, vibration and buckling of simply supported thick multilayered orthotropic plates: an evaluation of a new displacement model*. Journal of Sound and Vibration, Vol. 105, pp. 425-442.
- [9] Murakami H., 1986: *Laminated composite plate theory with improved in-plane responses*. ASME Journal of Applied Mechanics, Vol. 53, pp. 661-666.
- [10] Di Sciuva M., 1985: *Development of an anisotropic, multilayered, shear-deformable rectangular plate element*. Computers and Structures, Vol. 21(4), pp. 789-796.
- [11] Di Sciuva M., 1985: *Evaluation of some multilayered, shear-deformable plate elements*. Proceedings of the 26th Structures, Structural Dynamics and Materials Conference, AIAA/ASME/ASCE/AHS-Paper 85-0717, pp. 394-400.
- [12] Di Sciuva M., 1990: *Further refinement in the transverse shear deformation theory for multilayered composite plates*. Atti Accademia delle Scienze di Torino, Vol. 124(5-6), pp. 248-268.
- [13] Di Sciuva M., 1992: *Multilayered anisotropic plate models with continuous interlaminar stresses*. Composite Structures, Vol. 22(3), pp. 149-168.
- [14] Averill R. C., 1994: *Static and dynamic response of moderately thick laminated beams with damage*. Composites Engineering, Vol. 4(4), pp. 381-395.
- [15] Averill R. C. and Yuen Cheong Yip, 2006: *Development of simple, robust finite elements based on refined theories for thick laminated beams*. Computers & Structures, Vol. 59(3), pp. 529-546.
- [16] Umasree P. and Bhaskar K., 2006: *Analytical solutions for flexure of clamped rectangular cross-ply plates using an accurate zig-zag type higher-order theory*. Composite Structures, Vol. 74, pp. 426-439.
- [17] Mindlin R. D., 1951: *Influence of rotatory inertia and shear deformation on flexural motions of isotropic elastic plates*. ASME Journal of Applied Mechanics, Vol. 18, pp. 31-38.

- [18] Reissner E., 1945: *The effect of transverse shear deformation on the bending of elastic plates*. ASME Journal of Applied Mechanics, Vol. 12, pp. 69-77.
- [19] Pagano N. J., 1969: *Exact solutions for composite laminates in cylindrical bending*. Journal of Composite Materials, Vol. 3, pp. 398-411.
- [20] Di Sciuva M., Gherlone M. and Librescu L., 2002: *Implications of damaged interfaces and of other non-classical effects on the load carrying capacity of multilayered composite shallow shells*. International Journal of Non-Linear Mechanics, Vol. 37, pp. 851-867.
- [21] MSC/MD-NASTRAN: *Reference Guide, Version 2006.0*. MSC Software Corporation, Santa Ana, CA.

Appendix A. Stiffness coefficients in refined zigzag theory

Listed below are definitions of the stiffness coefficients that appear in the constitutive equations, Eqs. (47) and (48).

$$(A_{11}, B_{12}, D_{11}) \equiv \int_A E_x^{(k)} (1, z, z^2) dA \quad (\text{A1})$$

$$(B_{13}, D_{12}, D_{22}) \equiv \int_A E_x^{(k)} \phi^{(k)} (1, z, \phi^{(k)}) dA \quad (\text{A2})$$

$$(Q_{11}^\lambda, Q_{12}^\lambda, Q_{22}^\lambda) \equiv (Q + \lambda, -\lambda, \lambda) \quad (\text{A3})$$

and

$$Q \equiv \int_A G_{xz}^{(k)} (1 + \beta^{(k)})^2 dA \equiv GA \quad (\text{A4})$$

where the constants G and λ are defined in Eqs. (35) and (41), respectively. Note that a Timoshenko-type shear correction factor is not used within the present theory when modeling a heterogeneous cross-section. For homogeneous beams or laminated beams in which the shear moduli are the same (or nearly the same), the present theory reduces back to Timoshenko theory. In this case, it is appropriate to use the standard shear correction factor $k^2 = 5/6$ (for a rectangular cross-section) in the definition of the shear stress.

Appendix B. Cantilevered beam: Exact solution material coefficients

The exact solution in Eqs. (54) corresponds to the case $C_2/C_1 < 0$. For $C_2/C_1 > 0$, trigonometric functions define the exact solution (instead of hyperbolic functions), in which case some coefficients listed below would have different expressions.

$$C_1 \equiv \frac{\left((D_{12}^*)^2 - D_{11}^* D_{22}^* \right) Q_{11}^\lambda}{D_{12}^* Q_{11}^\lambda - D_{11}^* Q_{12}^\lambda}, \quad C_2 \equiv \frac{\left(Q_{11}^\lambda Q_{22}^\lambda - (Q_{12}^\lambda)^2 \right) D_{11}^*}{D_{12}^* Q_{11}^\lambda - D_{11}^* Q_{12}^\lambda}, \quad C_3 \equiv \frac{D_{22}^* Q_{11}^\lambda - D_{12}^* Q_{12}^\lambda}{D_{12}^* Q_{11}^\lambda - D_{11}^* Q_{12}^\lambda}, \quad (B1)$$

$$C_4 \equiv \frac{Q_{12}^\lambda}{Q_{11}^\lambda}, \quad C_5 \equiv \frac{D_{11}^*}{Q_{11}^\lambda}, \quad C_6 \equiv \frac{D_{12}^*}{Q_{11}^\lambda}, \quad C_7 \equiv \frac{B_{12}}{A_{11}}, \quad C_8 \equiv \frac{B_{13}}{A_{11}}, \quad R \equiv \sqrt{|C_2/C_1|}$$

$$D_{11}^* \equiv \frac{D_{11} A_{11} - (B_{12})^2}{A_{11}}, \quad D_{12}^* \equiv \frac{D_{12} A_{11} - B_{12} B_{13}}{A_{11}}, \quad D_{22}^* \equiv \frac{D_{22} A_{11} - (B_{13})^2}{A_{11}} \quad (B2)$$

Appendix C. Alternative derivation of zigzag function

An identical form of the zigzag function $\phi^{(k)}$ derived in Section 3.1 can be obtained by minimizing the shear strain energy for the case $\eta = 0$. Under this assumption, the transverse shear strain energy per unit length and width may be written as

$$S = \frac{1}{2} \int_{-h}^h G_{xz}^{(k)} (1 + \beta^{(k)}) \gamma (1 + \beta^{(k)}) \gamma dz = \frac{\gamma^2}{2} \sum_{k=1}^N G_{xz}^{(k)} (1 + \beta^{(k)})^2 2h^{(k)} \quad (C1)$$

Using Eq. (29) one obtains

$$S = \frac{\gamma^2}{2} \sum_{k=1}^N G_{xz}^{(k)} \left(1 + \frac{u^{(k)} - u^{(k-1)}}{2h^{(k)}} \right)^2 2h^{(k)} \quad (C2)$$

Minimizing S with respect to the unknown interface displacements $u^{(k)}$ yields

$$\frac{\partial S}{\partial u^{(k)}} = \frac{\gamma^2}{2} \left(G_{xz}^{(k)} 2h^{(k)} 2 \left(1 + \frac{u^{(k)} - u^{(k-1)}}{2h^{(k)}} \right) \frac{1}{2h^{(k)}} + G_{xz}^{(k+1)} 2h^{(k+1)} 2 \left(1 + \frac{u^{(k+1)} - u^{(k)}}{2h^{(k+1)}} \right) \frac{-1}{2h^{(k+1)}} \right) = 0 \quad (C3)$$

resulting in (for $k=1, \dots, N-1$)

$$G_{xz}^{(k)} \left(1 + \frac{u^{(k)} - u^{(k-1)}}{2h^{(k)}} \right) = G_{xz}^{(k+1)} \left(1 + \frac{u^{(k+1)} - u^{(k)}}{2h^{(k+1)}} \right) \quad (C4)$$

The above relationship is identical to that of Eq. (33).

Appendix D. Reference finite element model for the cantilevered beam

The cantilevered beam is analyzed using a two-dimensional plane-stress model discretized with QUAD8 elements based on serendipity shape functions [21]. The discretization involves a uniform mesh having 40 elements in the direction of the beam thickness and 200 along its length, with a total of 8000 elements, and nearly 49,000 degrees-of-freedom. The tip transverse force F is modeled by way of a parabolic shear traction $f(z)$ ($f(\pm h) = 0$) distributed along the free end of the beam, producing the total shear force of $F = \int_{-h}^h f(z) dz$. The displacements are computed at the nodes, whereas the strains and stresses are evaluated at the element centroids.

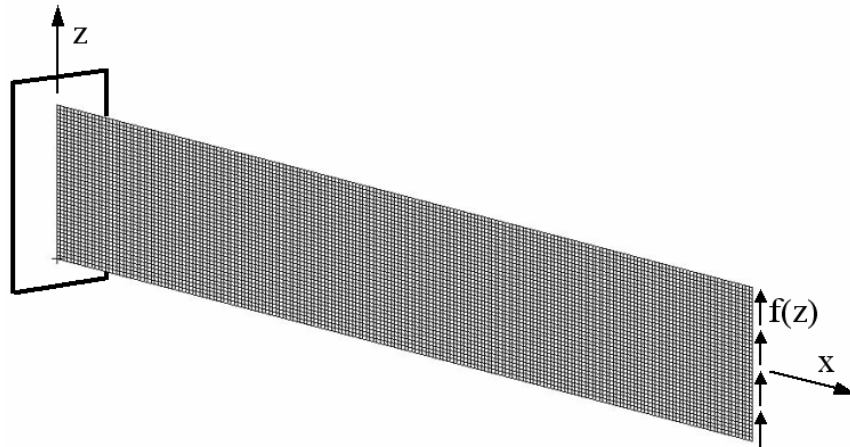


Figure 27. Geometry, boundary conditions, and loading for the cantilevered beam modeled as a two-dimensional plane-stress problem using MSC/NASTRAN[®].

REPORT DOCUMENTATION PAGE

*Form Approved
OMB No. 0704-0188*

The public reporting burden for this collection of information is estimated to average 1 hour per response, including the time for reviewing instructions, searching existing data sources, gathering and maintaining the data needed, and completing and reviewing the collection of information. Send comments regarding this burden estimate or any other aspect of this collection of information, including suggestions for reducing this burden, to Department of Defense, Washington Headquarters Services, Directorate for Information Operations and Reports (0704-0188), 1215 Jefferson Davis Highway, Suite 1204, Arlington, VA 22202-4302. Respondents should be aware that notwithstanding any other provision of law, no person shall be subject to any penalty for failing to comply with a collection of information if it does not display a currently valid OMB control number.

PLEASE DO NOT RETURN YOUR FORM TO THE ABOVE ADDRESS.

1. REPORT DATE (DD-MM-YYYY) 01-11-2007		2. REPORT TYPE Technical Publication		3. DATES COVERED (From - To)	
4. TITLE AND SUBTITLE Refinement of Timoshenko Beam Theory for Composite and Sandwich Beams Using Zigzag Kinematics				5a. CONTRACT NUMBER	
				5b. GRANT NUMBER	
				5c. PROGRAM ELEMENT NUMBER	
6. AUTHOR(S) Tessler, Alexander; Di Sciuva, Marco; and Gherlone, Marco				5d. PROJECT NUMBER	
				5e. TASK NUMBER	
				5f. WORK UNIT NUMBER 984754.02.07.07.15.04	
7. PERFORMING ORGANIZATION NAME(S) AND ADDRESS(ES) NASA Langley Research Center Hampton, VA 23681-2199			8. PERFORMING ORGANIZATION REPORT NUMBER L-19411		
Department of Aeronautics and Space Engineering Politecnico di Torino Corso Duca degli Abruzzi, 24 10129, Torino, Italy					
9. SPONSORING/MONITORING AGENCY NAME(S) AND ADDRESS(ES) National Aeronautics and Space Administration Washington, DC 20546-0001				10. SPONSORING/MONITOR'S ACRONYM(S) NASA	
				11. SPONSORING/MONITORING REPORT NUMBER NASA/TP-2007-215086	
12. DISTRIBUTION/AVAILABILITY STATEMENT Unclassified-Unlimited Subject Categories: 24 and 39 Availability: NASA CASI (301) 621-0390					
13. SUPPLEMENTARY NOTES An electronic version can be found at http://ntrs.nasa.gov					
14. ABSTRACT A new refined theory for laminated-composite and sandwich beams that contains the kinematics of the Timoshenko Beam Theory as a proper baseline subset is presented. This variationally consistent theory is derived from the virtual work principle and employs a novel piecewise linear zigzag function that provides a more realistic representation of the deformation states of transverse shear flexible beams than other similar theories. This new zigzag function is unique in that it vanishes at the top and bottom bounding surfaces of a beam. The formulation does not enforce continuity of the transverse shear stress across the beam's cross-section, yet is robust. Two major shortcomings that are inherent in the previous zigzag theories, shear-force inconsistency and difficulties in simulating clamped boundary conditions, and that have greatly limited the utility of these previous theories are discussed in detail. An approach that has successfully resolved these shortcomings is presented herein. This new theory can be readily extended to plate and shell structures, and should be useful for obtaining accurate estimates of structural response of laminated composites.					
15. SUBJECT TERMS Timoshenko beam theory; Zigzag kinematics; Shear deformation; Composite beams; Sandwich beams; Virtual work principle					
16. SECURITY CLASSIFICATION OF:			17. LIMITATION OF ABSTRACT UU	18. NUMBER OF PAGES 45	19a. NAME OF RESPONSIBLE PERSON STI Help Desk (email: help@sti.nasa.gov)
a. REPORT U	b. ABSTRACT U	c. THIS PAGE U			19b. TELEPHONE NUMBER (Include area code) (301) 621-0390